[1,4]-Cycloaddition and C–X Bond Activation Reactions of monovalent Group 13 diyls

Hanns Micha Weinert,[a] Pratima Dhawan,[a] Timo Freese,[a] Christoph Wölper,[a] and Stephan Schulz,[a,b]]*

[a] Dr. H. M. Weinert (ORCID: 0000-0003-1957-9430), T. Freese, Dr. C. Wölper, Prof. Dr. S. Schulz (ORCID: 0000-0003-2896-4488)
Institute of Inorganic Chemistry, University of Duisburg-Essen, Universitätsstraße 5-7, 45141 Essen, Germany
E-mail: stephan.schulz@uni-due.de; Homepage: https://www.uni-due.de/ak_schulz/index_en.php
[b] Center for Nanointegration Duisburg-Essen (CENIDE), University of Duisburg-Essen, Carl-Benz-Straße 199, 47057 Duisburg, Germany

Content

A) Spectroscopic Characterization

Table S1. ^{1}H and ^{13}C NMR chemical shifts δ [ppm] of selected moieties of **1**–**10** and for LGa and LIn for reference.

	ArNCCH_3	ArNCCH_3]	γ-CH	Ga/In-CH_x
LGa[1]	1.67(24.0)	(163.5)	5.19(99.6)	/
LIn[2][a]	1.72(24.3)	(163.8)	5.00(98.1)	
1	1.55(23.5)	(168.8)	4.74(95.8)	1.12(20.5)
2	1.55, 1.52 (23.9, 23.4)	(169.4, 168.8)	4.74(96.3)	5.57, 1.07 (80.0, 15.6)
3	1.56, 1.52 (24.5, 24.4)	(170.8, 170.6)	4.76 (97.2)	not observed
4	1.57, 1.56 (25.1–24.6)	(171.5, 171.5)	4.72 (96.6)	not observed
5	1.56 (23.4)	(169.6)	4.87 (97.6)	1.94 (19.2)
6	1.56 (24.0)	(170.4)	4.77 (86.9)	2.15 (19.9)
7	1.57 (23.5)	(169.4)	4.92 (97.9)	0.47 (3.5)
8	1.58 (24.1)	(170.1)	4.83 (97.1)	0.67 (5.7)
9	1.60		5.15	1.99
9[b]	1.94		5.58	1.95
10[b]	2.16		6.10	2.47

[a] toluene-d_8; [b] DCM-d_2.

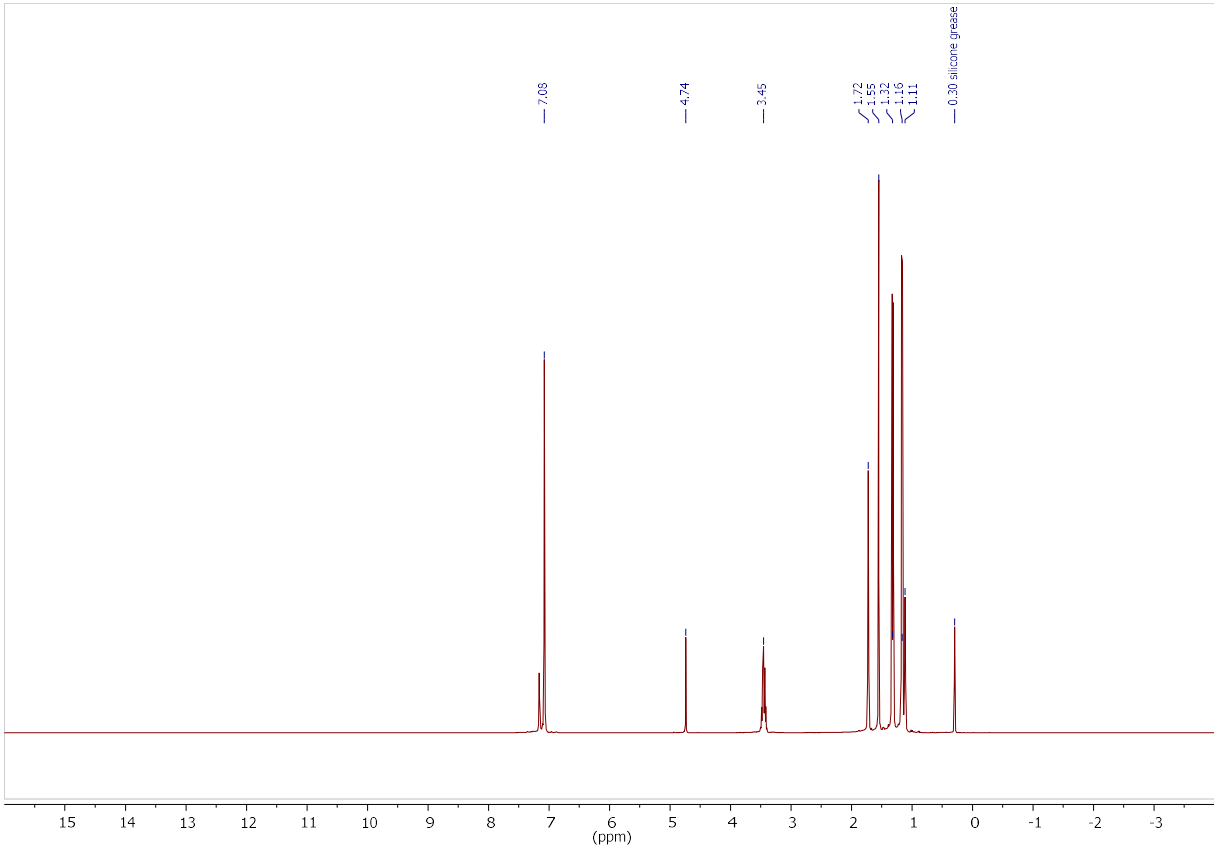

Fig. S1. ^{1}H NMR spectrum (400 MHz, C_6D_6, 25 °C) of LGa(C_6H_{10}) (**1**).

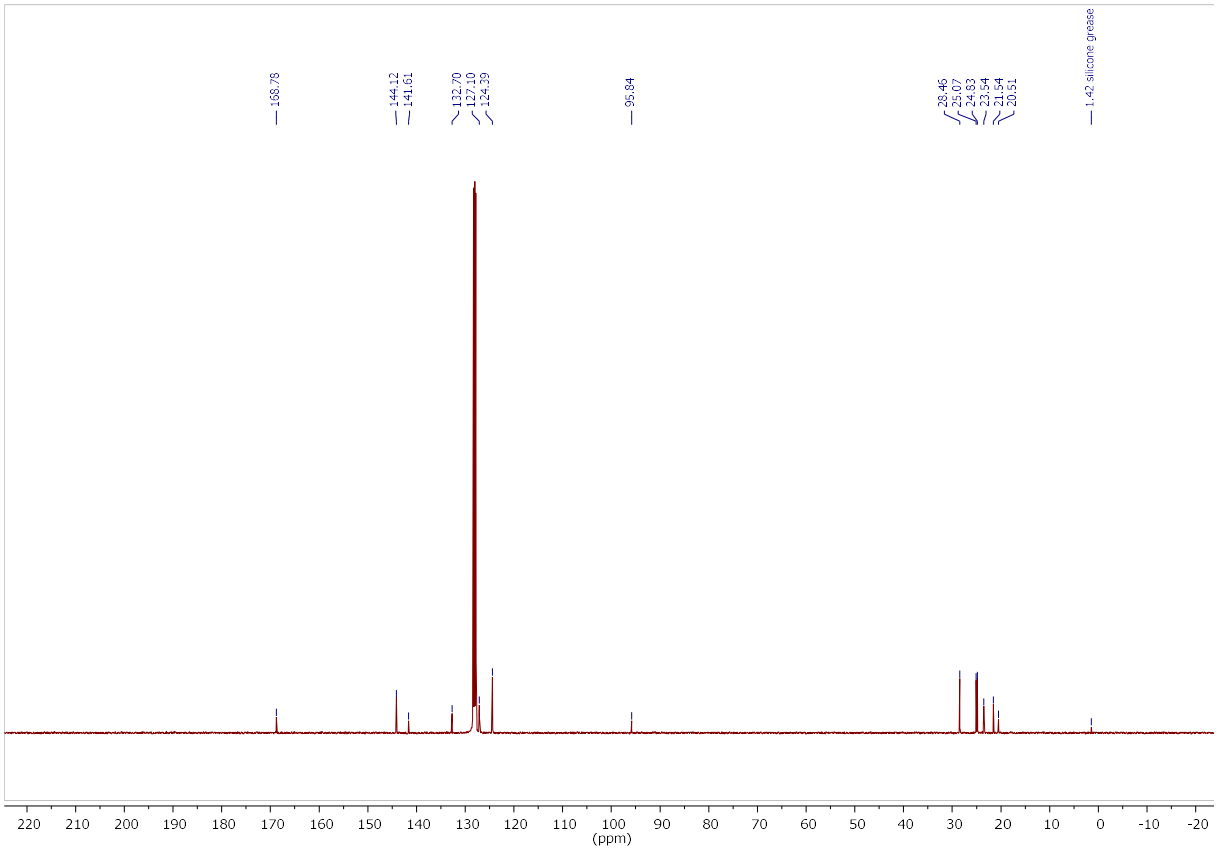

Fig. S2. ^{13}C NMR spectrum (100.6 MHz, C_6D_6, 25 °C) of LGa(C_6H_{10}) (**1**).

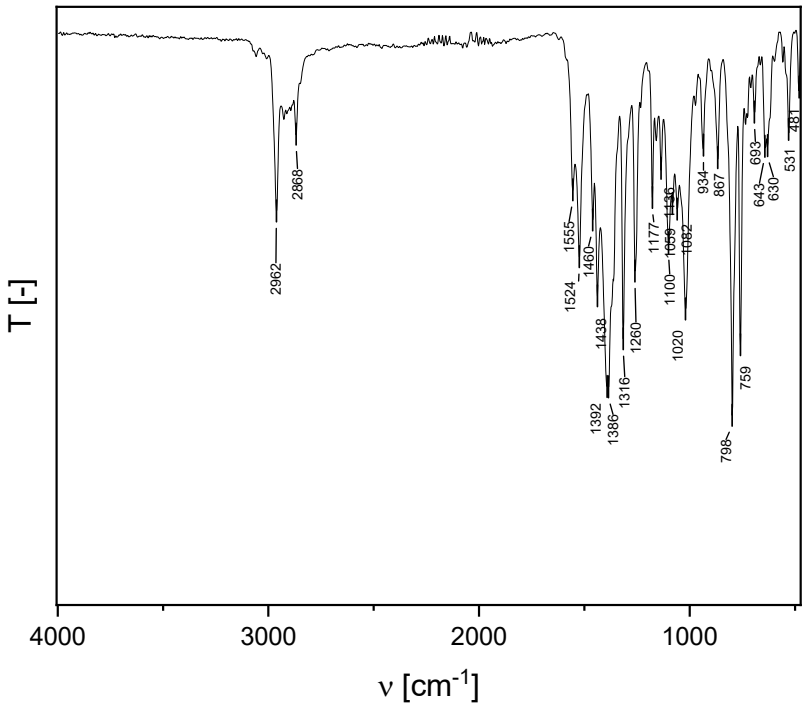

Fig. S3. ATR-IR spectrum of $LGa(C_6H_{10})$ (**1**).

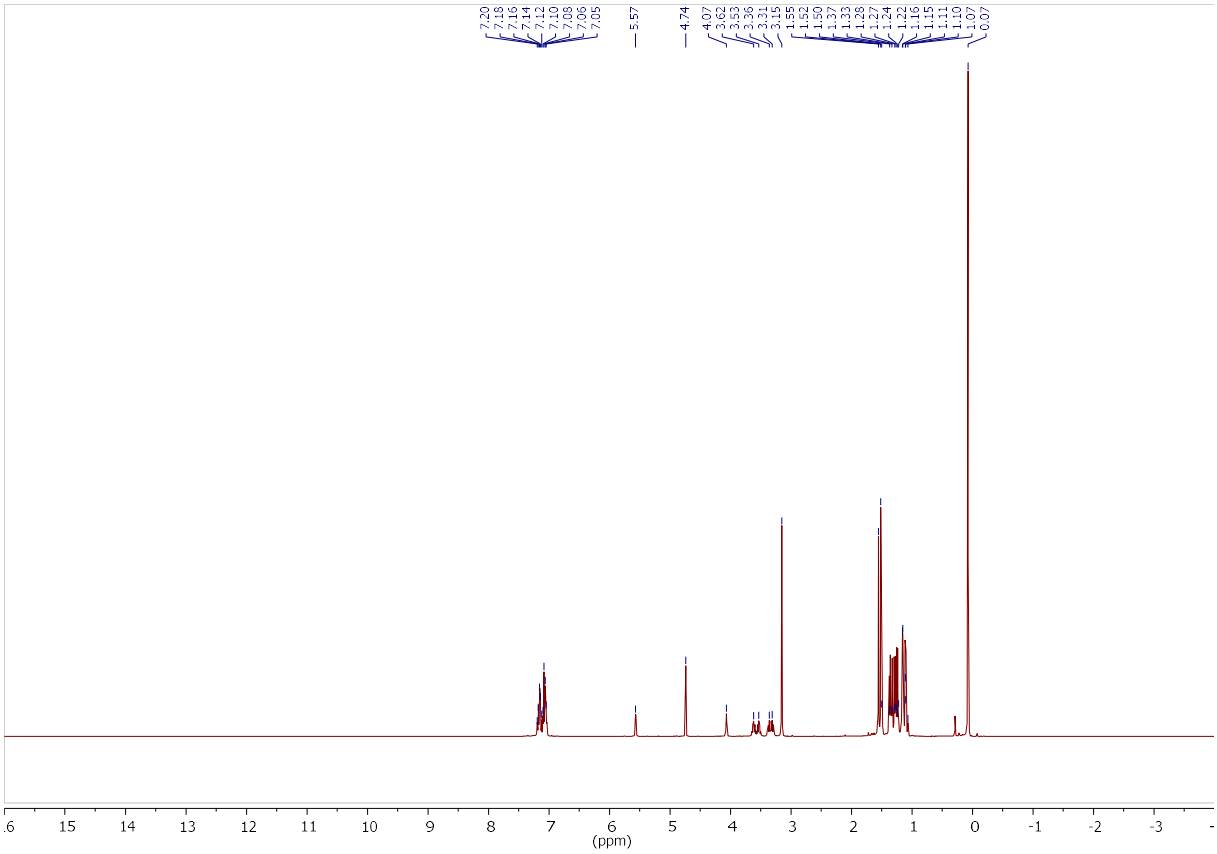

Fig. S4. ^{1}H NMR spectrum (400 MHz, C_6D_6, 25 °C) of $LGa(C_8H_{16}O_2Si)$ (**2**).

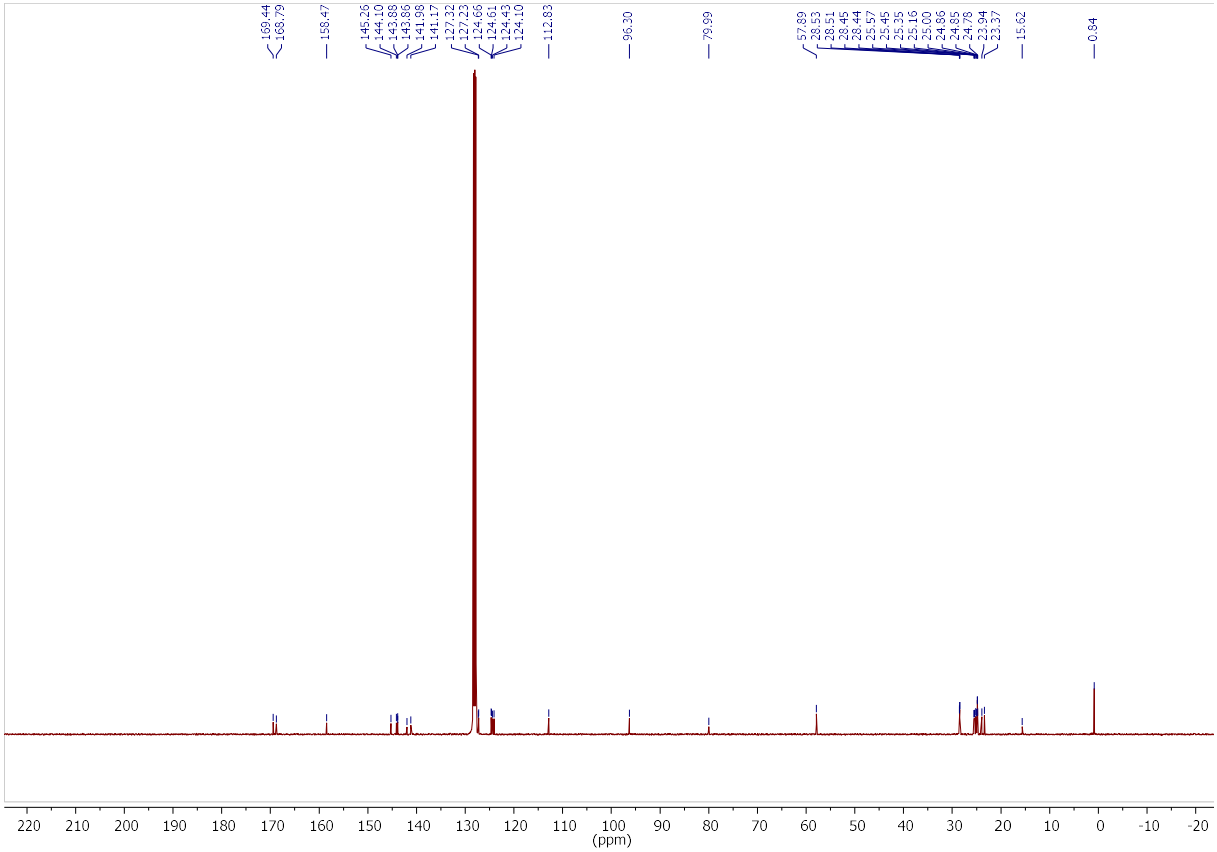

Fig. S5. ^{13}C NMR spectrum (100.6 MHz, C_6D_6, 25 °C) of LGa($C_8H_{16}O_2Si$) (**2**).

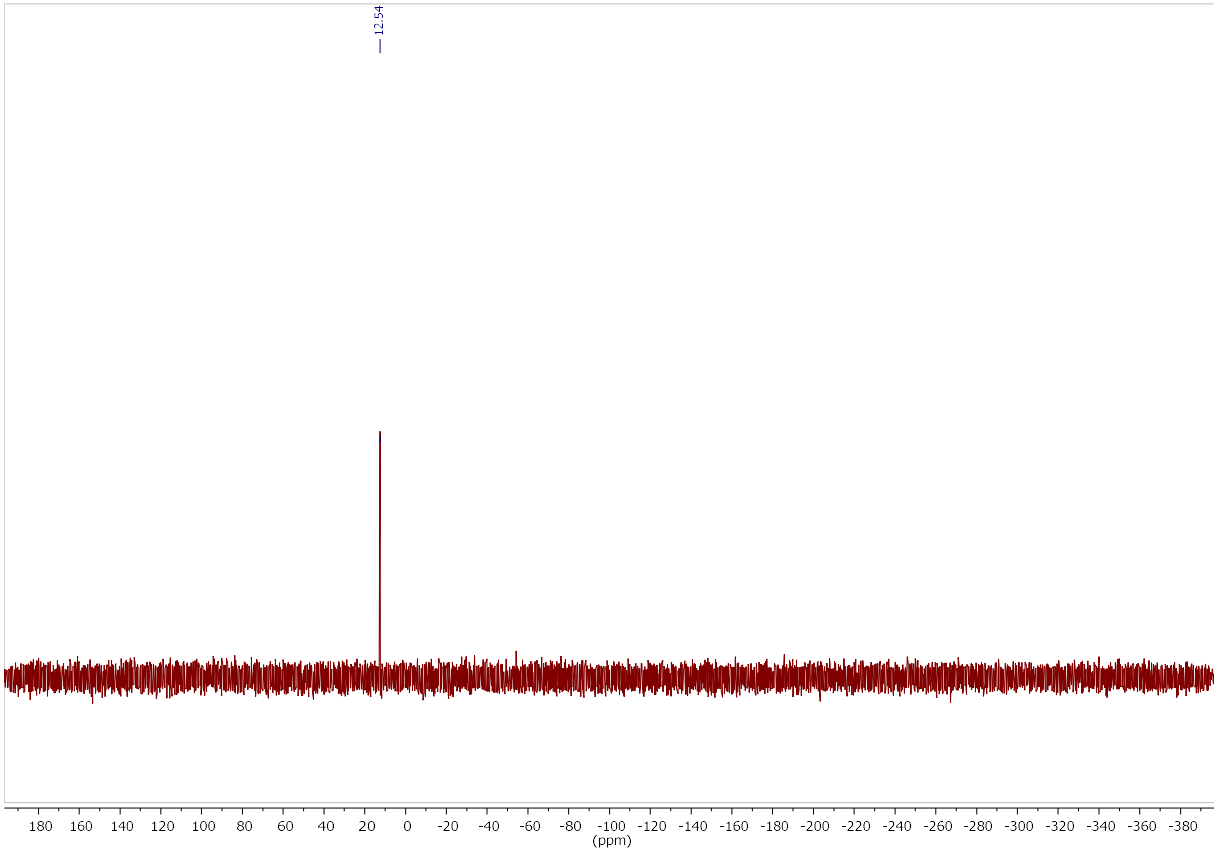

Fig. S6. DEPT ^{29}Si NMR spectrum (79.5 MHz, C_6D_6, 25 °C) of LGa($C_8H_{16}O_2Si$) (**2**).

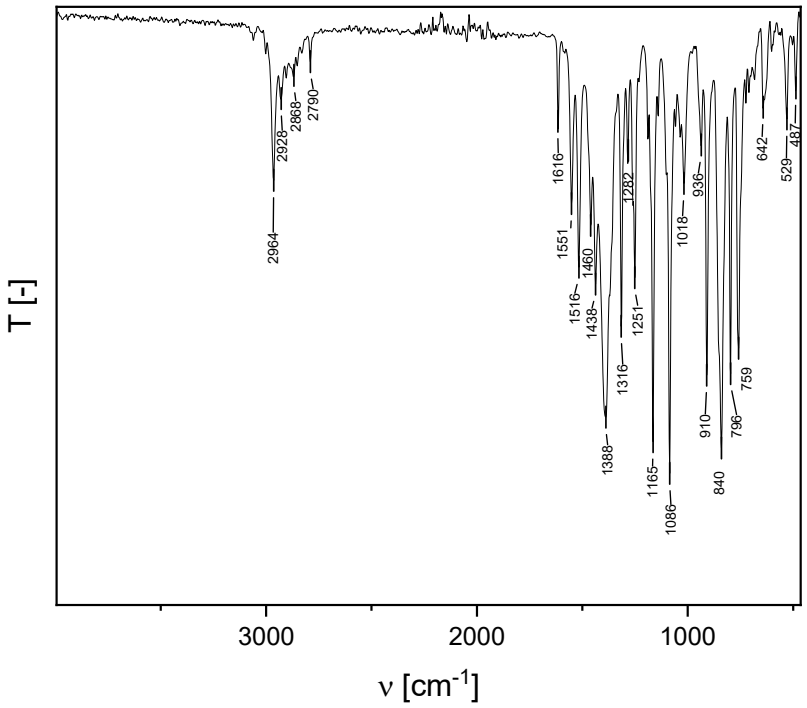

Fig. S7. ATR-IR spectrum of LGa($C_8H_{16}O_2Si$) (**2**).

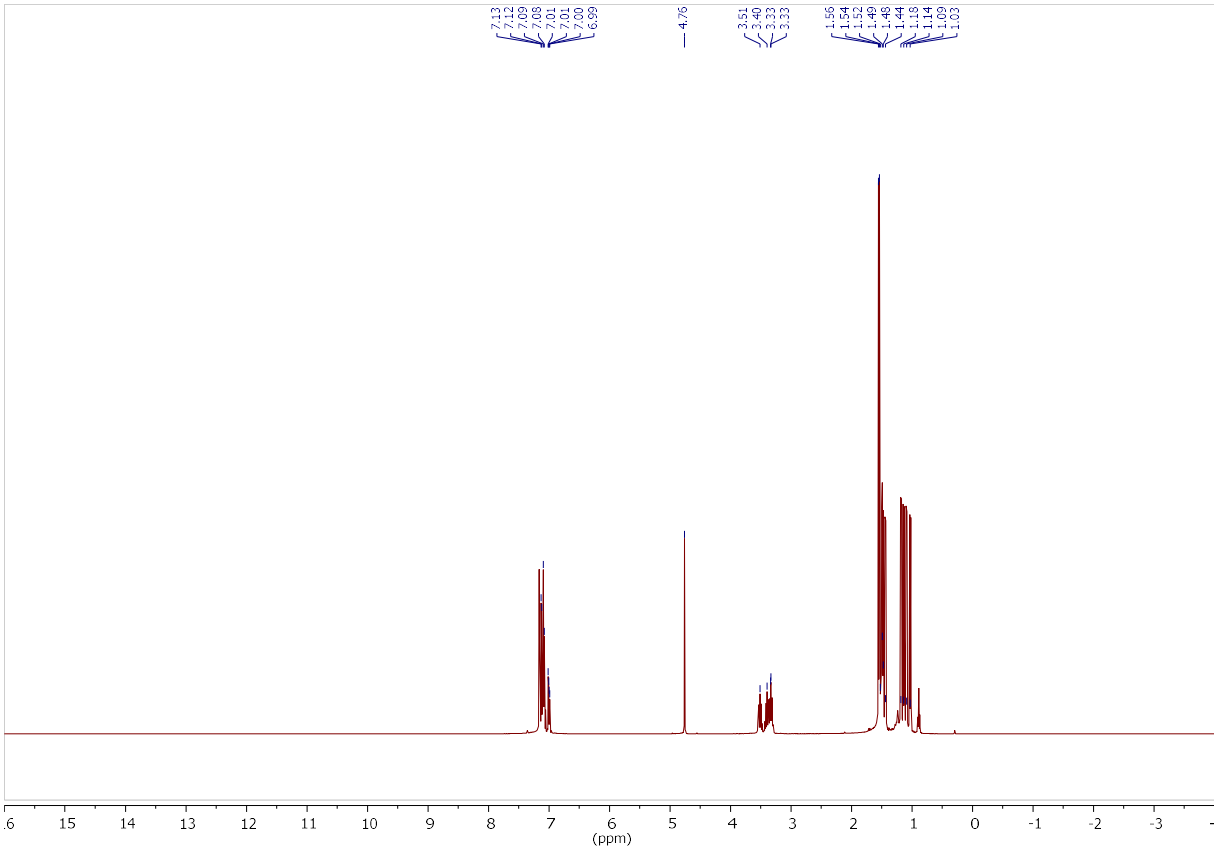

Fig. S8. ^{1}H NMR spectrum (400 MHz, C_6D_6, 25 °C) of L(Cl)Ga(C_4Cl_5) (**3**).

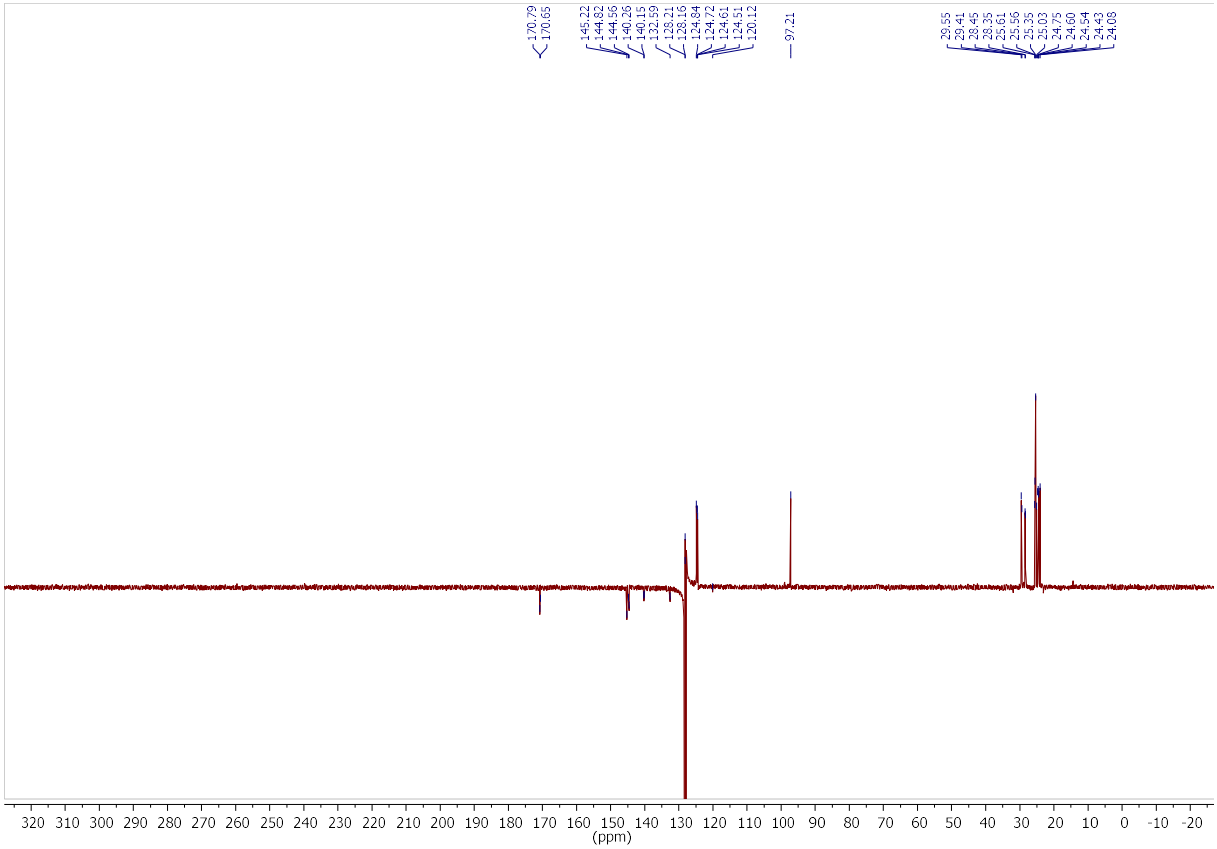

Fig. S9. DEPTQ ^{13}C NMR spectrum (100.6 MHz, C_6D_6, 25 °C) of L(Cl)Ga(C_4Cl_5) (**3**).

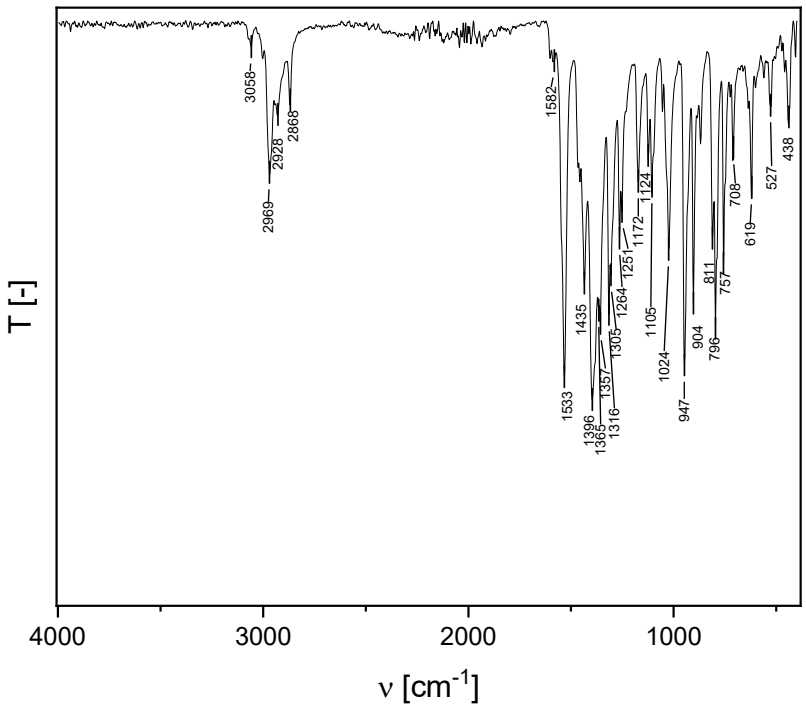

Fig. S10. ATR-IR spectrum of L(Cl)Ga(C_4Cl_5) (**3**).

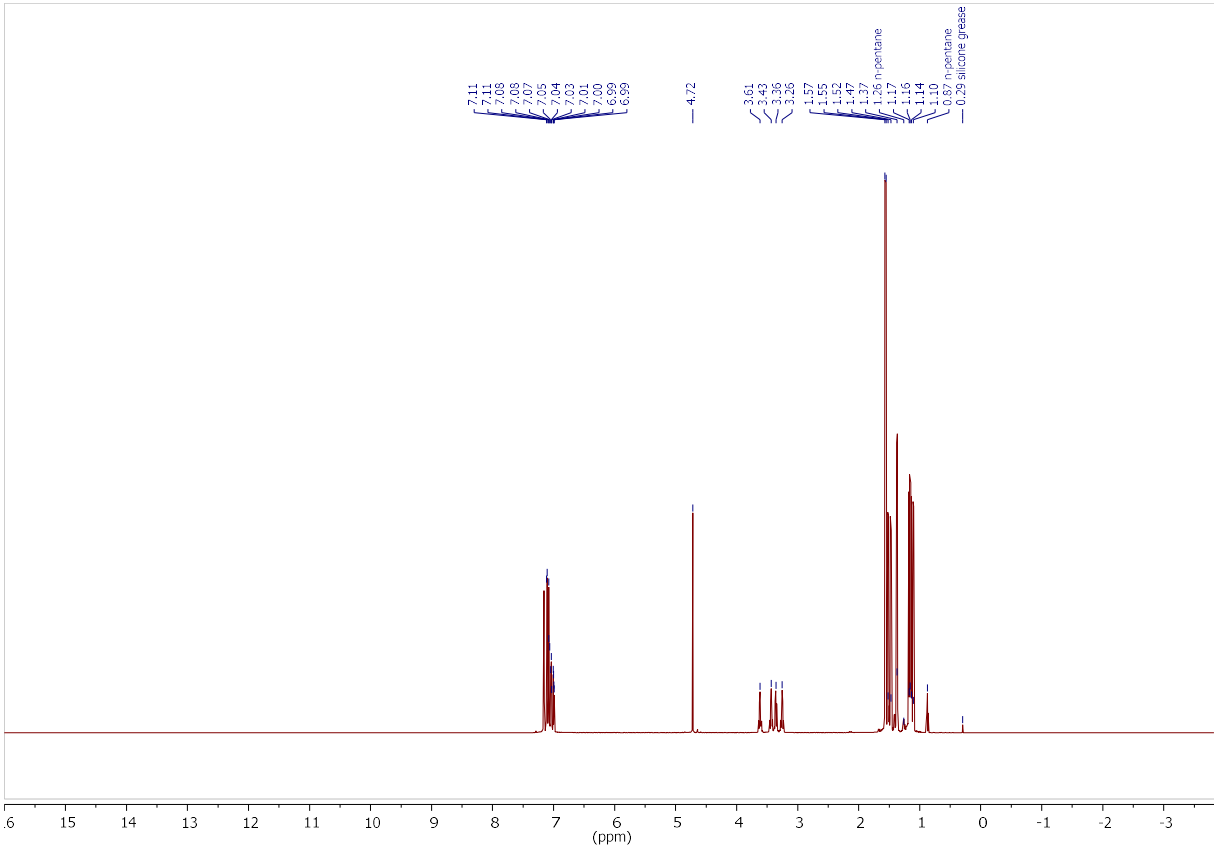

Fig. S11. ^{1}H NMR spectrum (600 MHz, C_6D_6, 25 °C) of L(Cl)In(C_4Cl_5) (**4**).

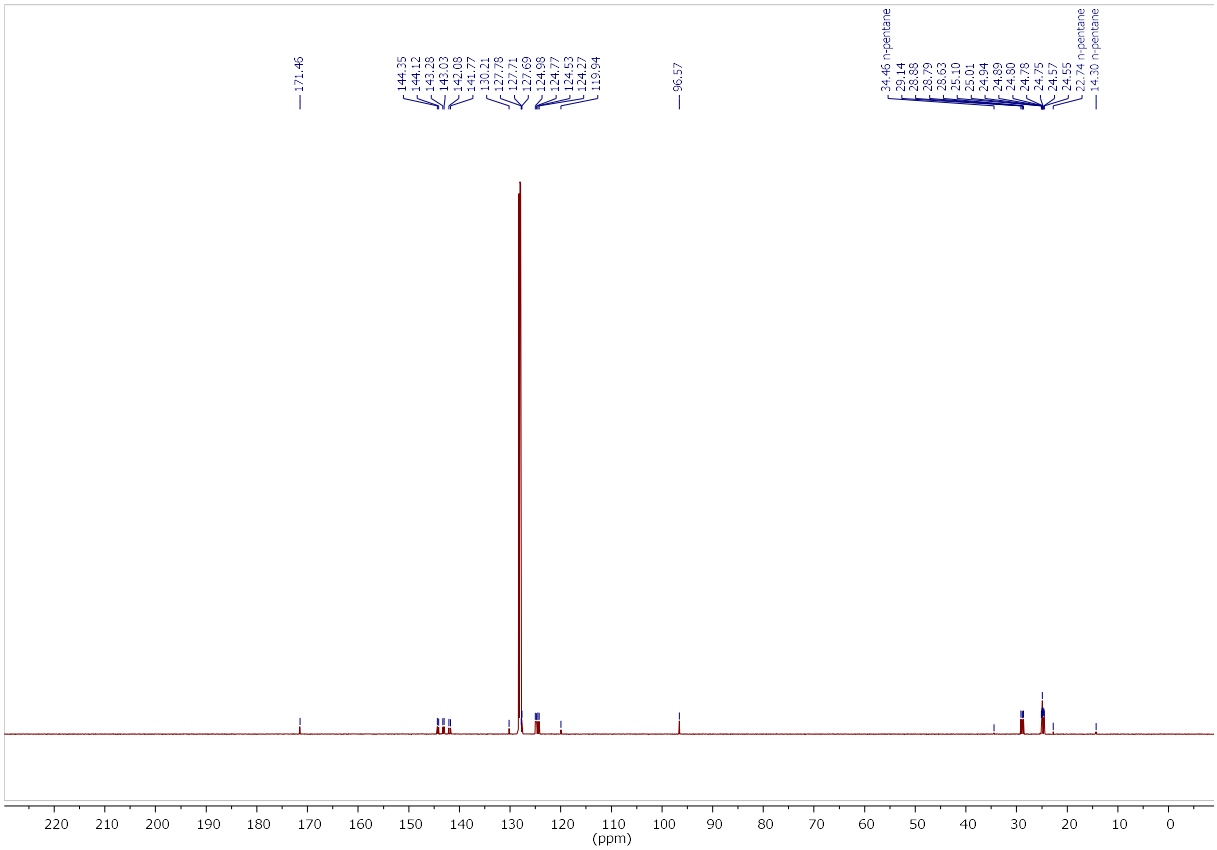

Fig. S12. ^{13}C NMR spectrum (150.9 MHz, C_6D_6, 25 °C) of L(Cl)In(C_4Cl_5) (**4**).

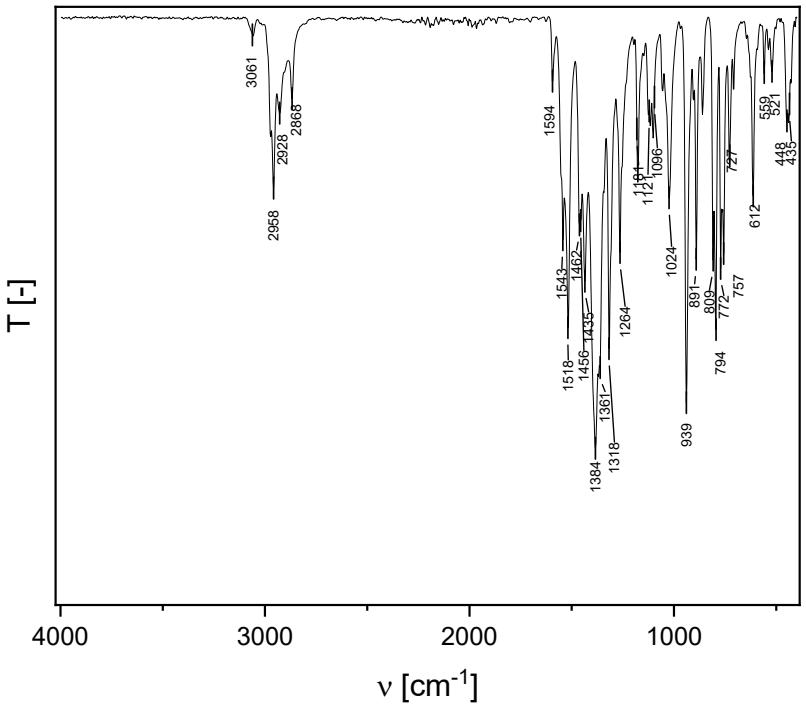

Fig. S13. ATR-IR spectrum of L(Cl)In(C_4Cl_5) (**4**).

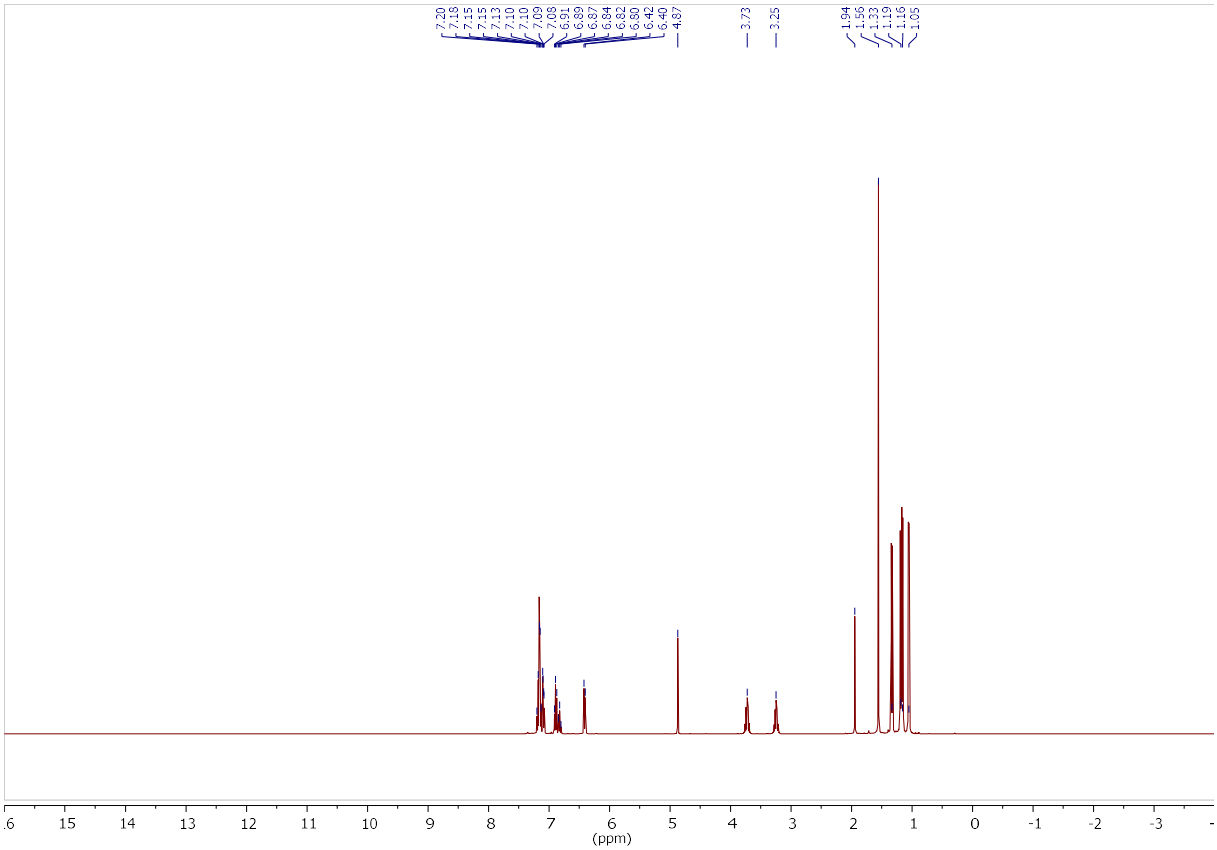

Fig. S14. ^{1}H NMR spectrum (400 MHz, C_6D_6, 25 °C) of L(Cl)Ga($CH_2C_6H_5$) (**5**).

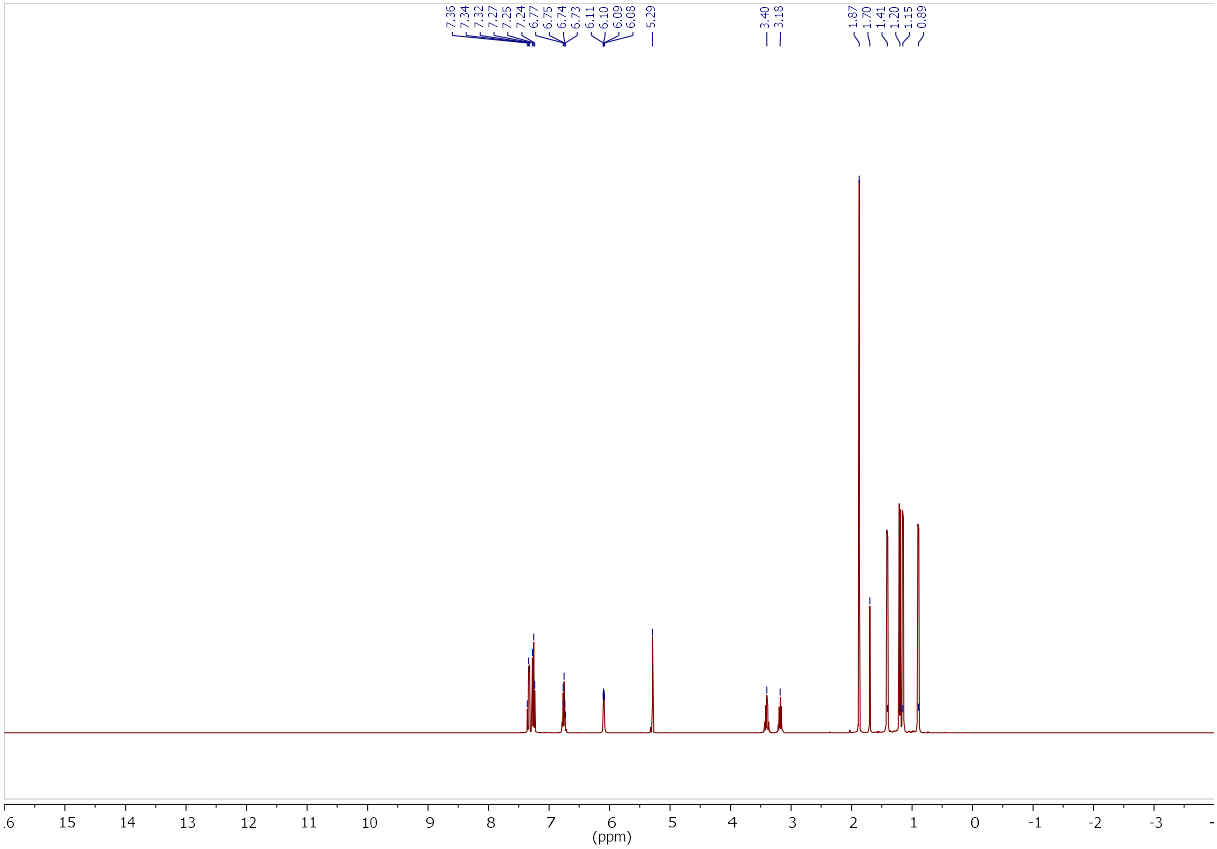

Fig. S15. ^{1}H NMR spectrum (400 MHz, DCM-d_2, 25 °C) of L(Cl)Ga($CH_2C_6H_5$) (**5**).

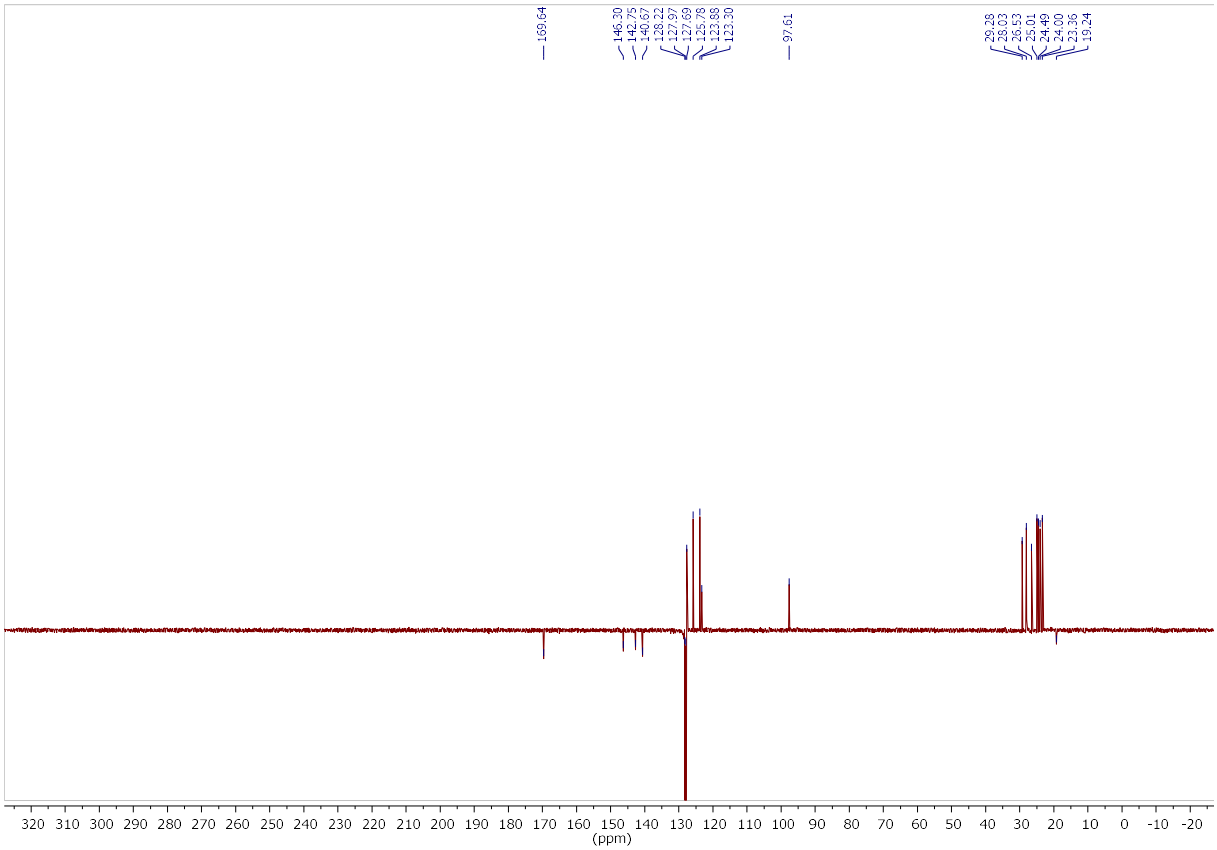

Fig. S16. DEPTQ ^{13}C NMR spectrum (100.6 MHz, C_6D_6, 25 °C) of L(Cl)Ga($CH_2C_6H_5$) (**5**).

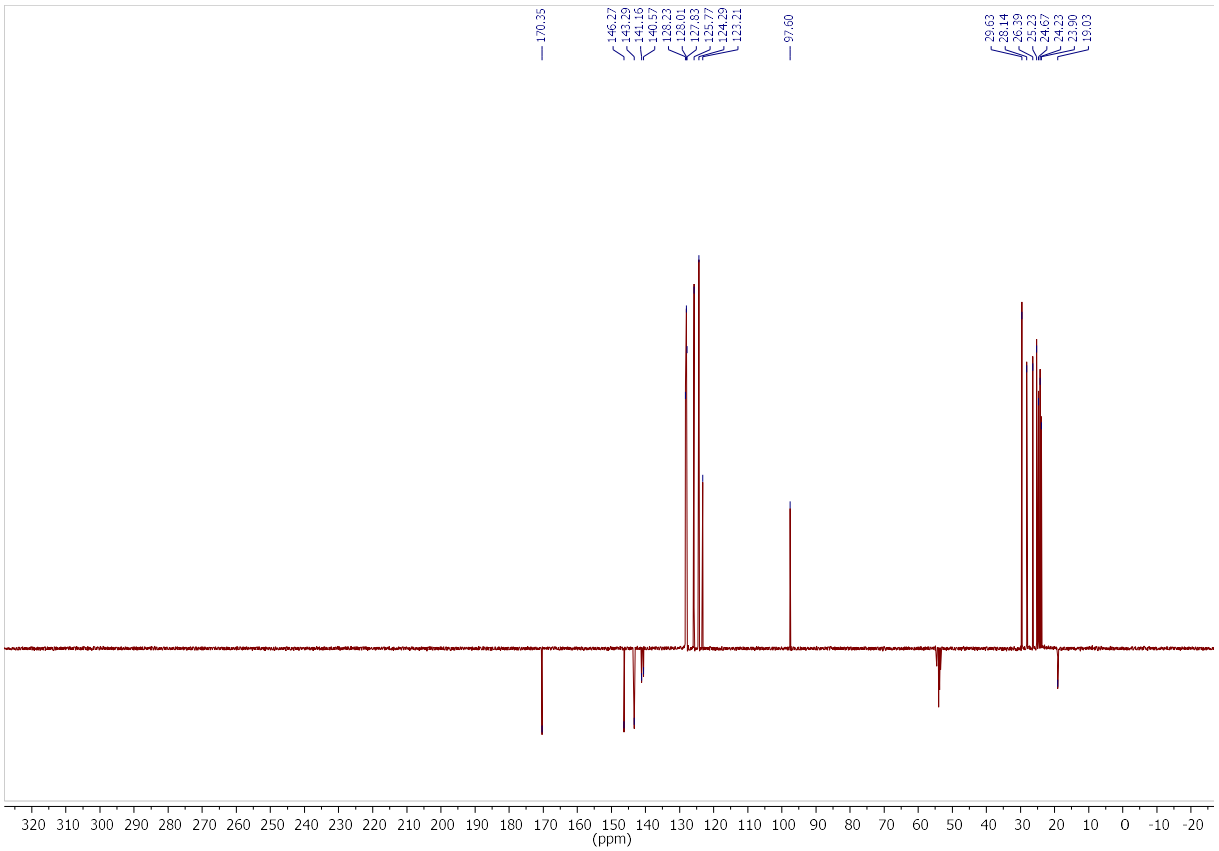

Fig. S17. DEPTQ ^{13}C NMR spectrum (100.6 MHz, DCM-d_2, 25 °C) of L(Cl)Ga($CH_2C_6H_5$) (**5**).

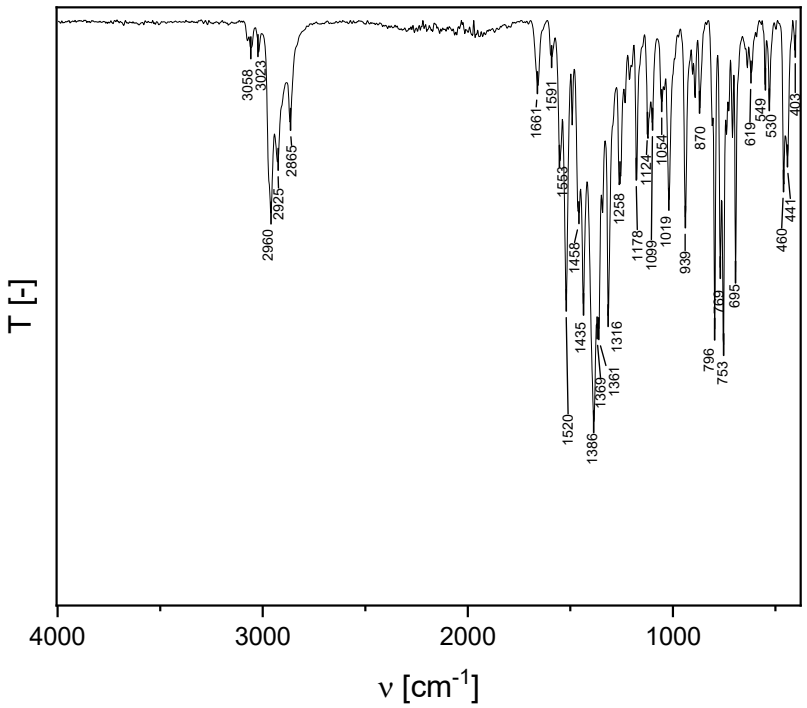

Fig. S18. ATR-IR spectrum of L(Cl)Ga($CH_2C_6H_5$) (**5**).

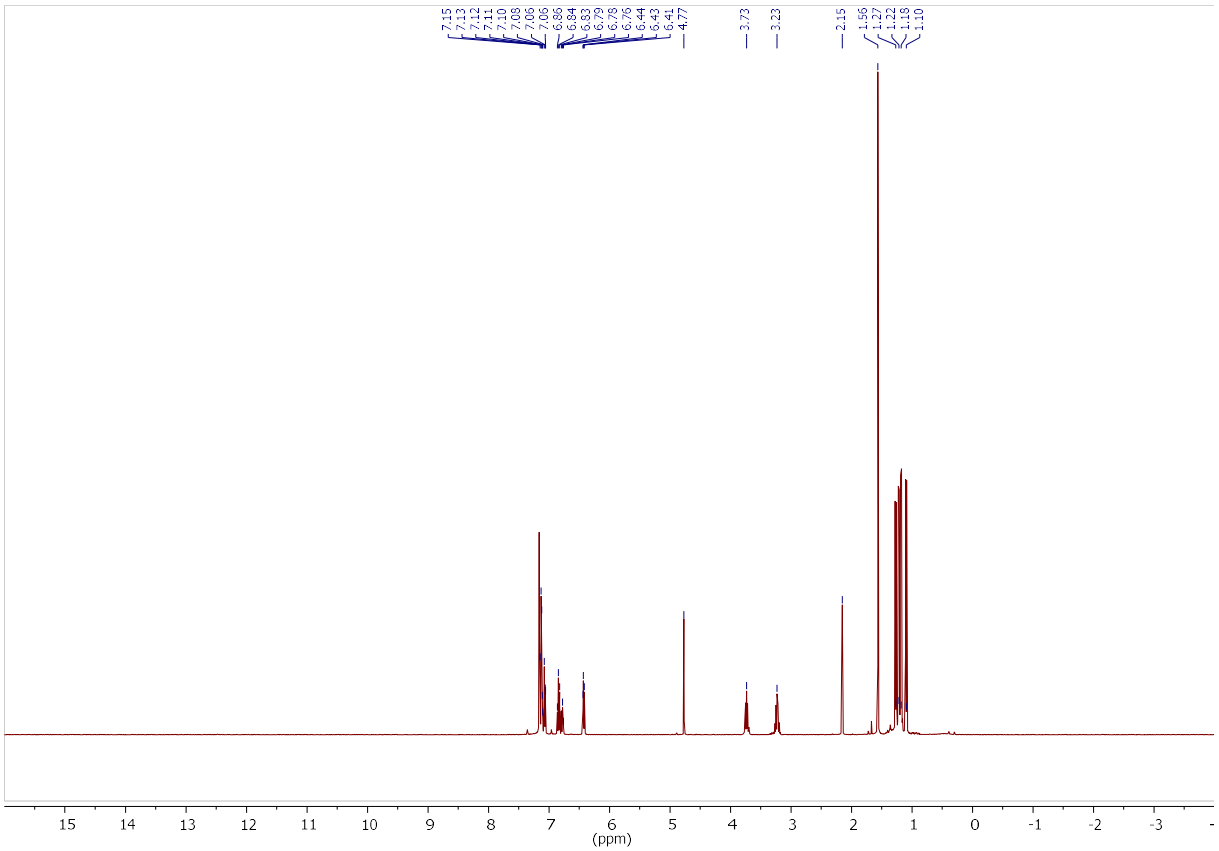

Fig. S19. ^{1}H NMR spectrum (400 MHz, C_6D_6, 25 °C) of L(Cl)In($CH_2C_6H_5$) (**6**).

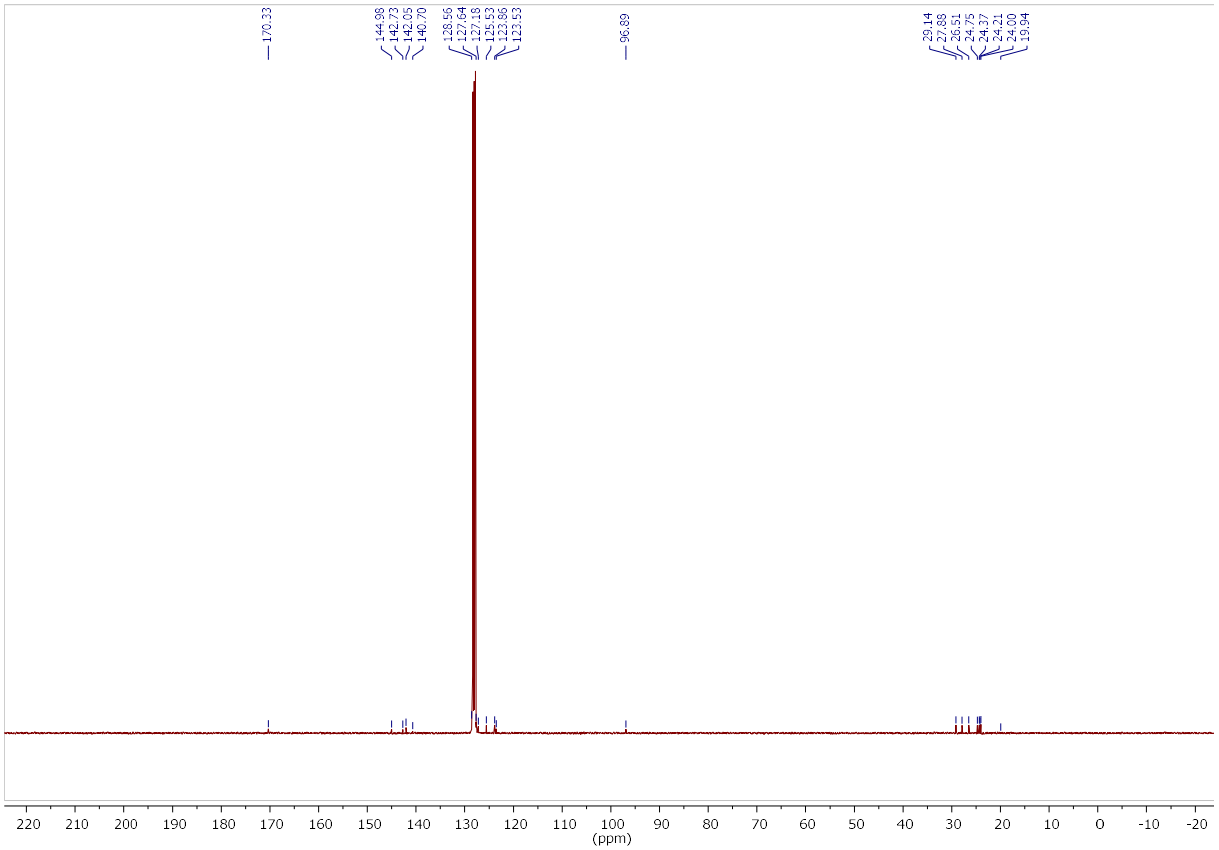

Fig. S20. ^{13}C NMR spectrum (100.6 MHz, C_6D_6, 25 °C) L(Cl)In($CH_2C_6H_5$) (**6**).

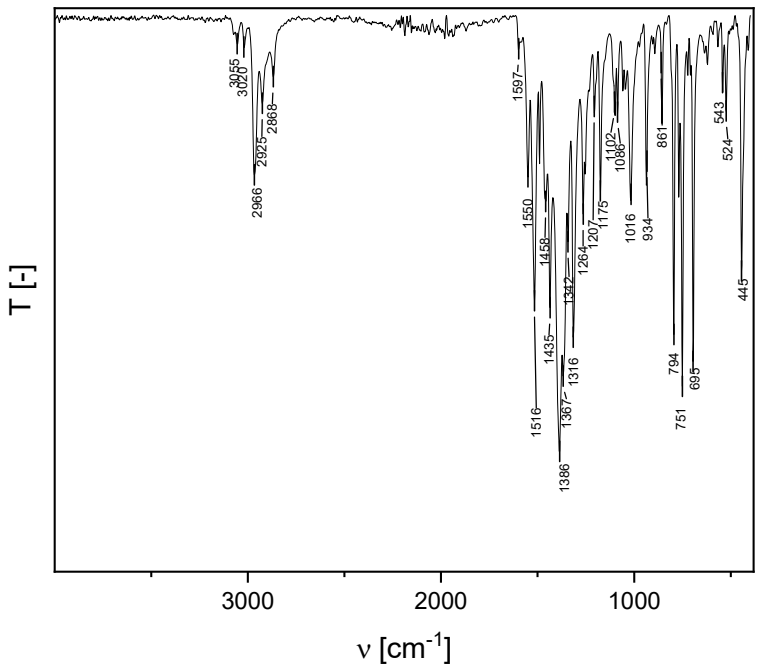

Fig. S21. ATR-IR spectrum of L(Cl)In($CH_2C_6H_5$) (**6**).

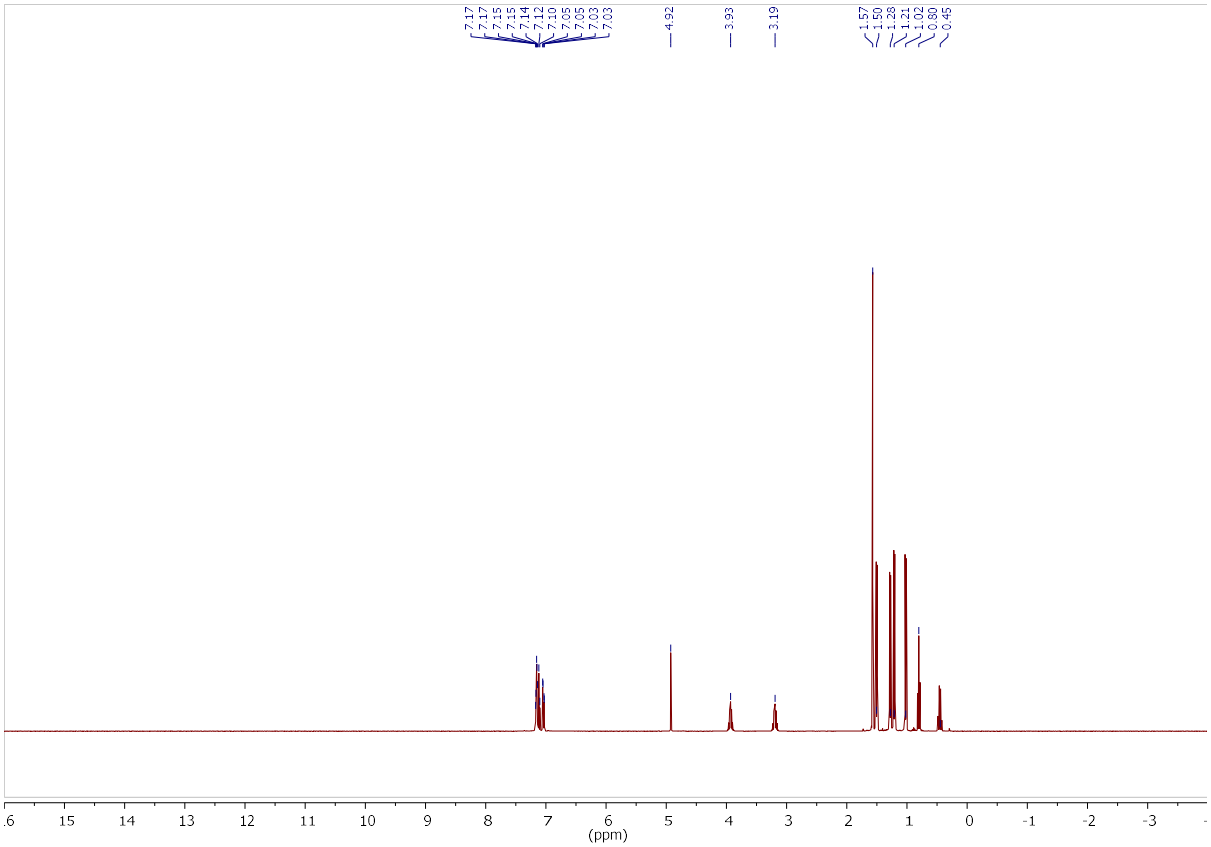

Fig. S22. ^{1}H NMR spectrum (400 MHz, C_6D_6, 25 °C) of L(Br)Ga(CH_2CH_3) (**7**).

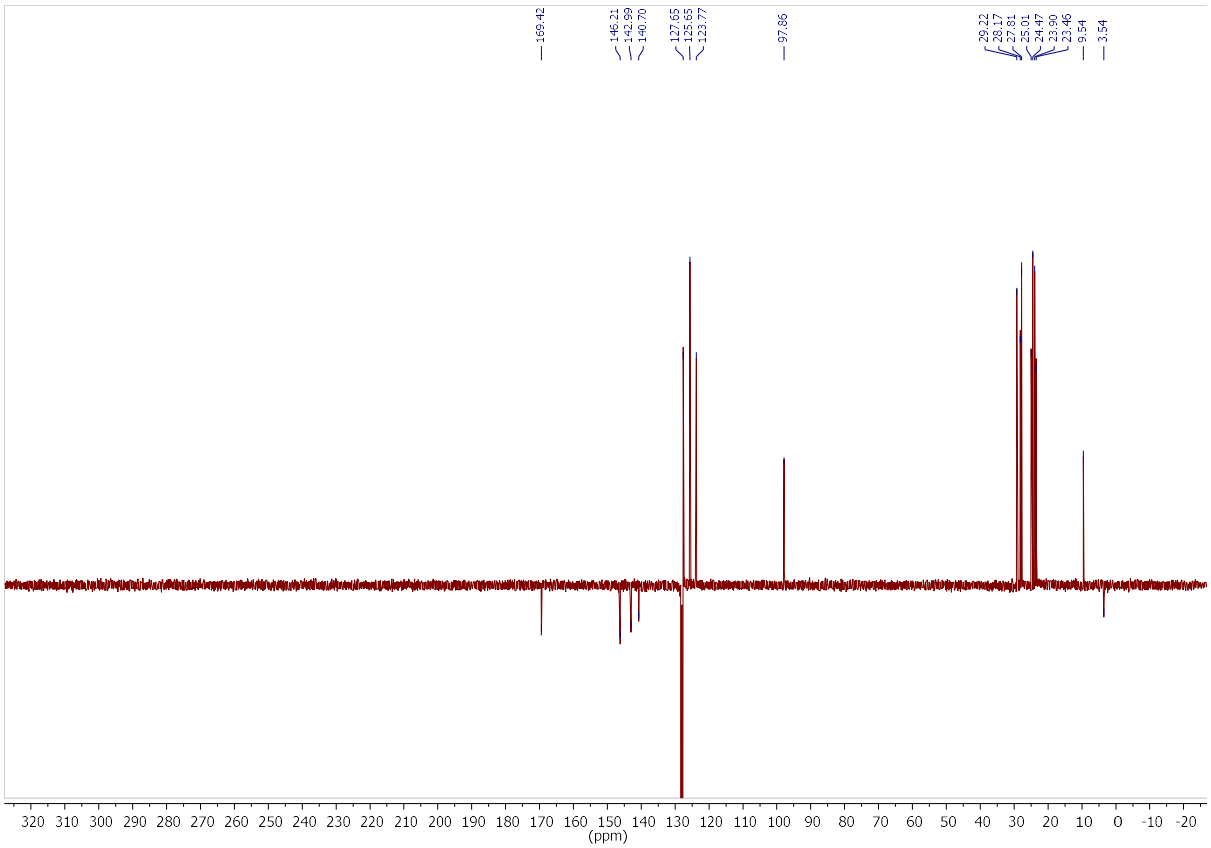

Fig. S23. DEPTQ ^{13}C NMR spectrum (100.6 MHz, DCM-d_2, 25 °C) of L(Br)Ga(CH_2CH_3) (**7**).

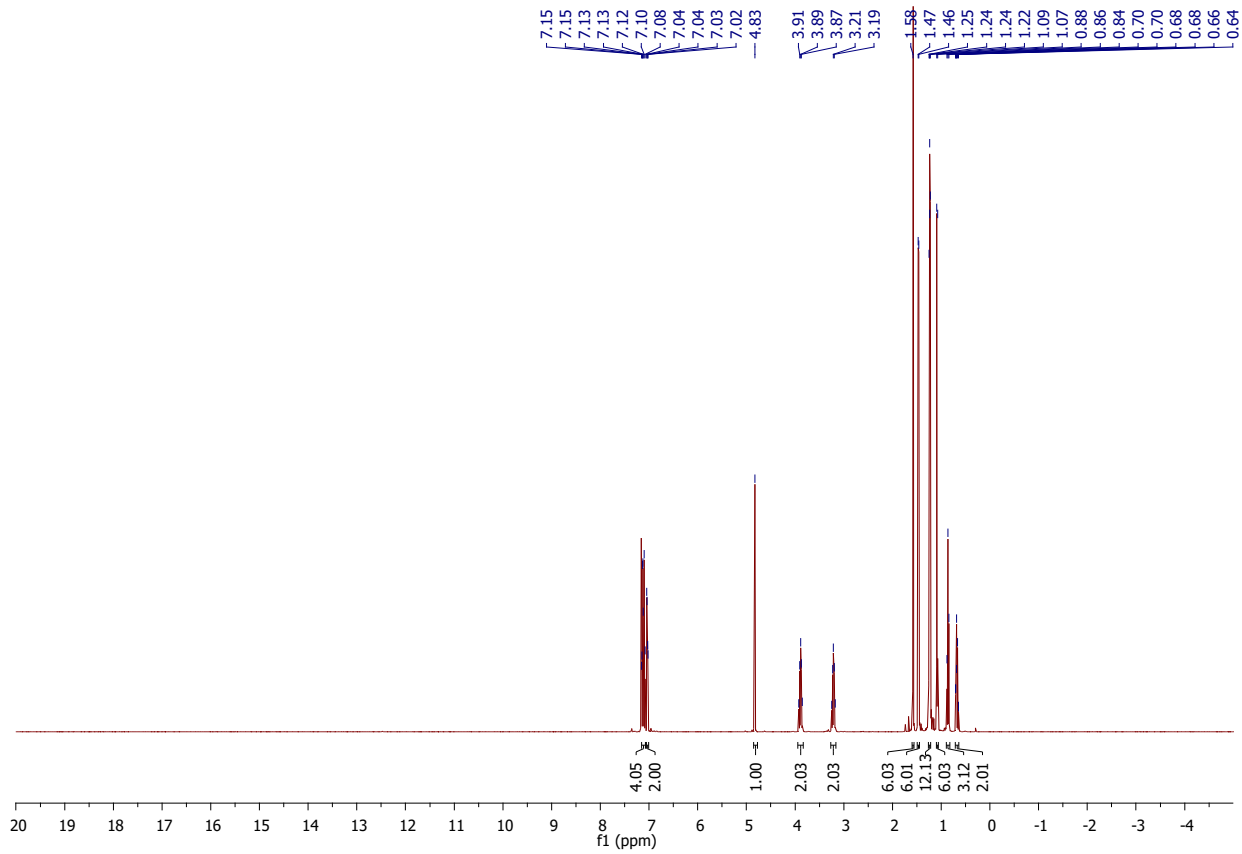

Fig. S24. ^1H NMR spectrum (400 MHz, C_6D_6, 25 °C) of L(Br)In(CH_2CH_3) (**8**).

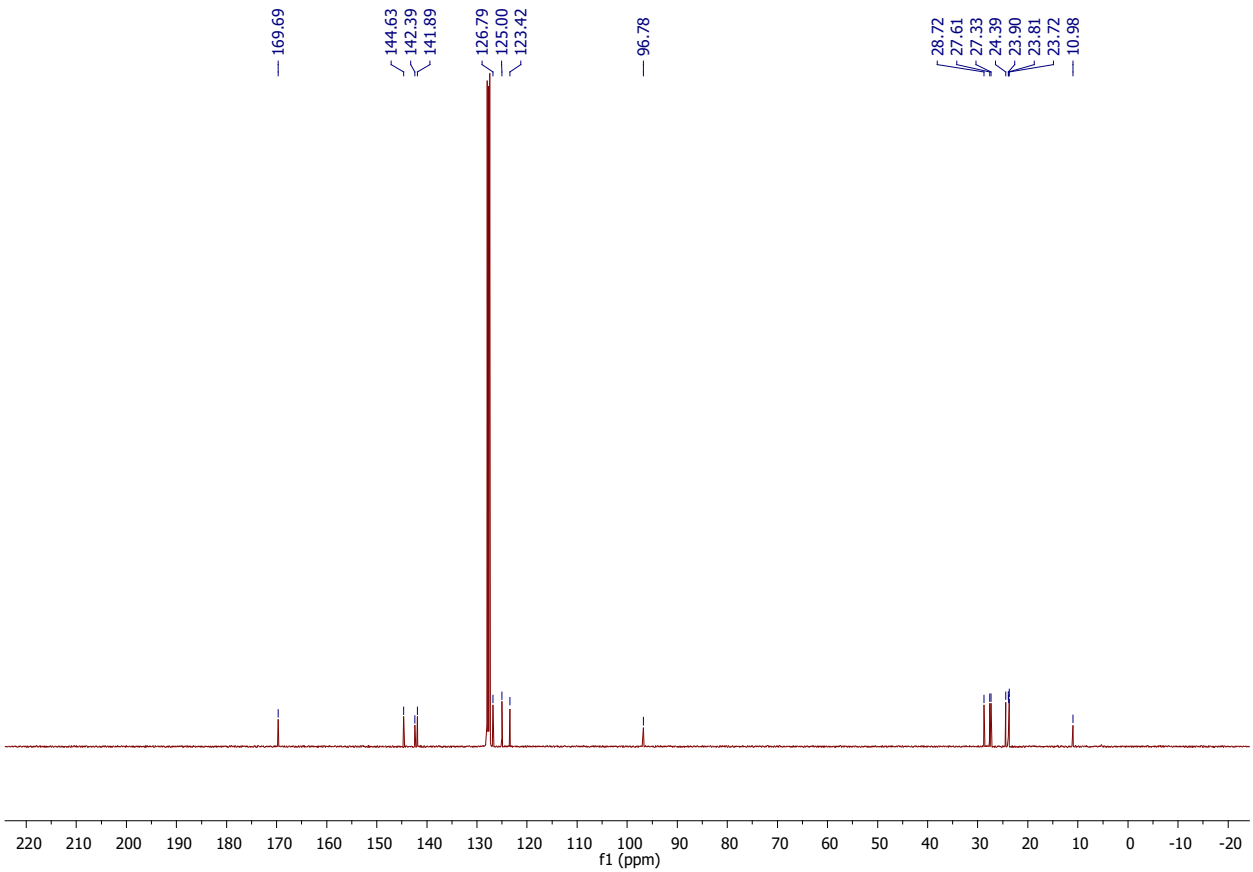

Fig. S25. ^{13}C NMR spectrum (100.6 MHz, C_6D_6, 25 °C) L(Br)In(CH_2CH_3) (**8**).

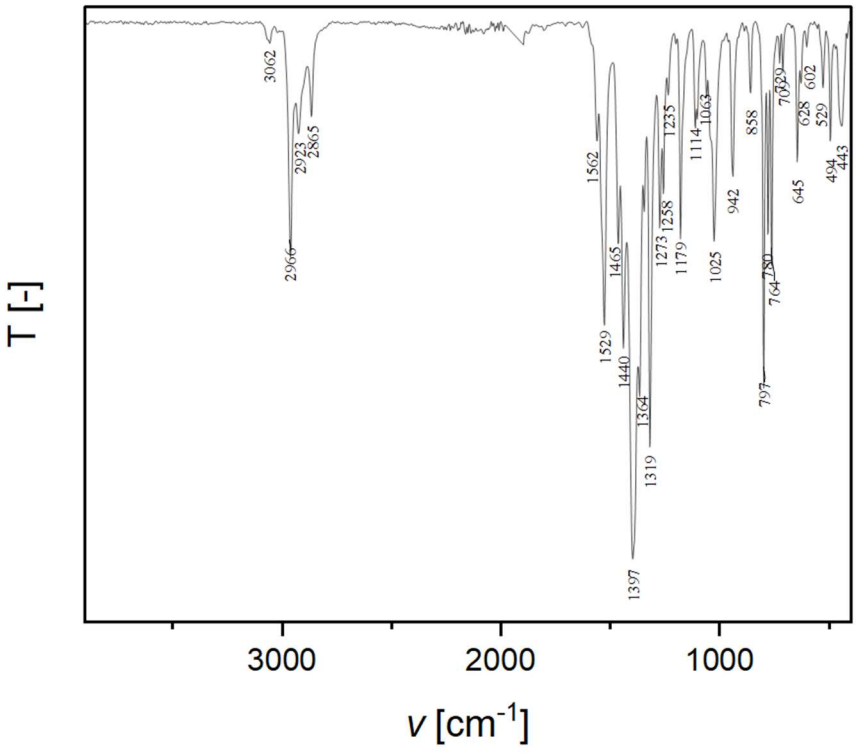

Fig. S26. AaTR-IR spectrum of L(Br)In(CH_2CH_3) (**8**).

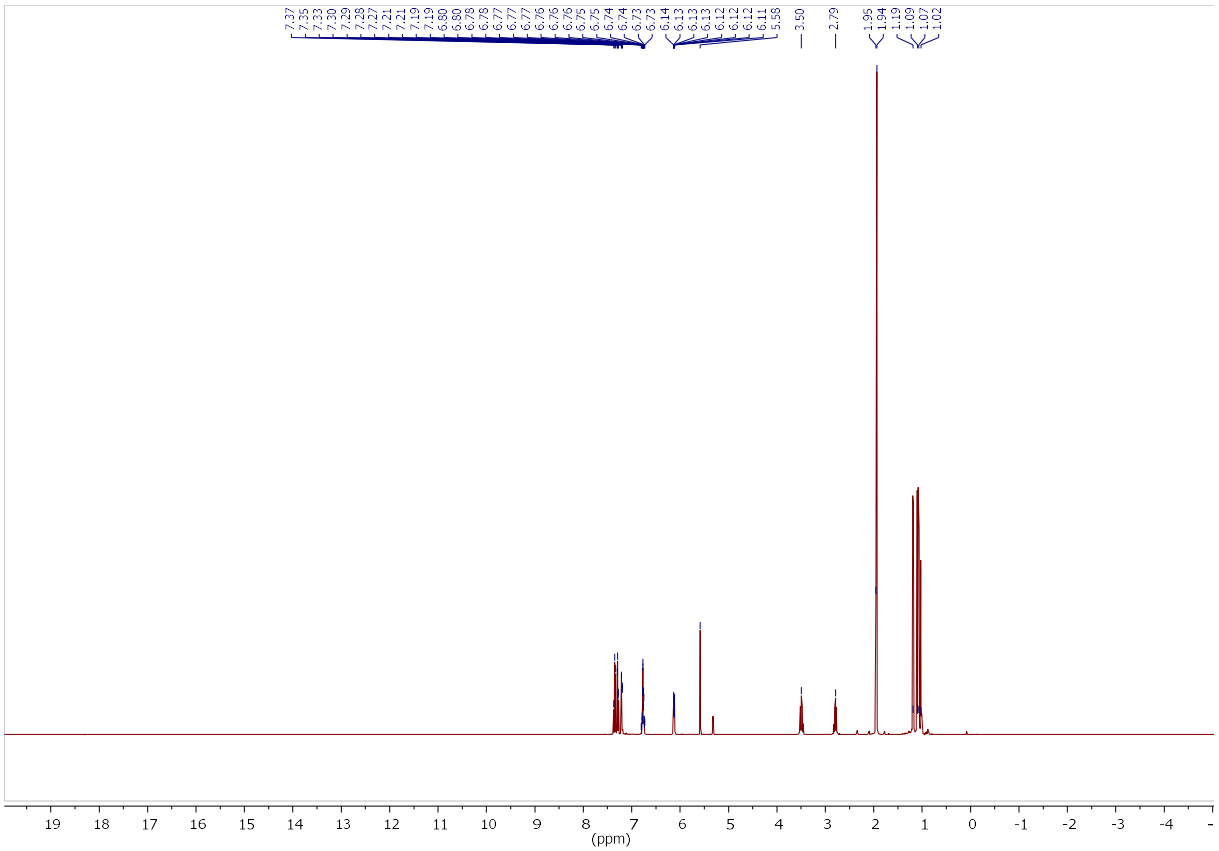

Fig. S27. ^{1}H NMR spectrum (400 MHz, DCM-d_2, 25 °C) of L(TfO)Ga($CH_2C_6H_5$) (**9**).

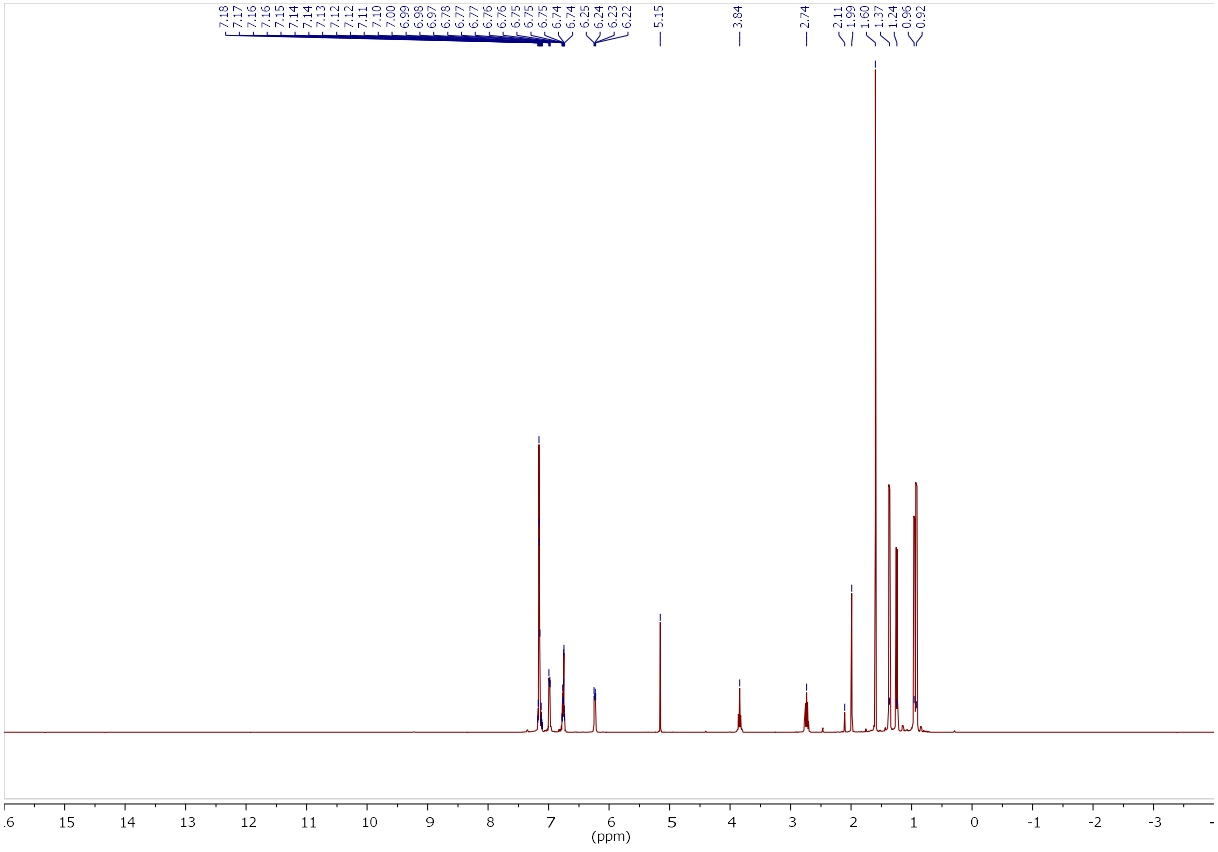

Fig. S 28. ^{1}H NMR spectrum (400 MHz, C_6D_6, 25 °C) of L(TfO)Ga($CH_2C_6H_5$) (**9**).

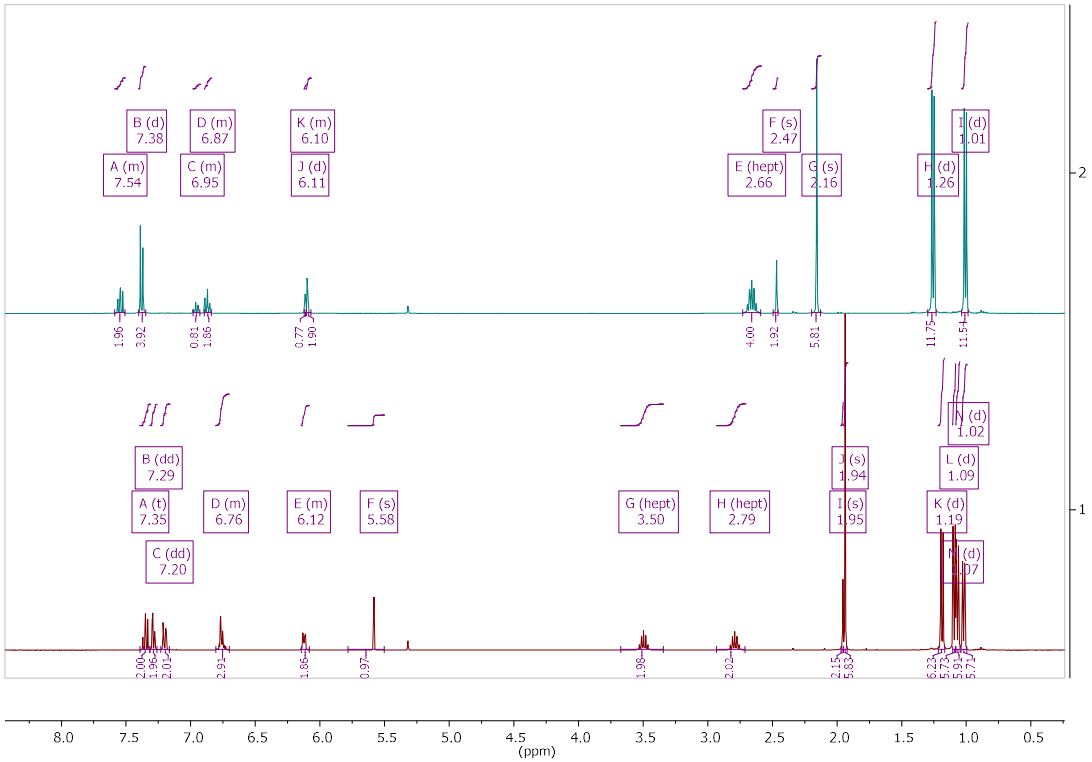

Fig. S29. ^{1}H NMR spectrum (400 MHz, DCM-d_2, 25 °C) of the reaction of L(TfO)Ga($CH_2C_6H_5$) (**9**) with NaB(C_6F_5)$_4$. Bottom, only **11**, top, after the addition of NaB(C_6F_5)$_4$. The formation of [LGa($CH_2C_6H_5$)][B(C_6F_5)$_4$] (**10**) is strongly indicated by the increased symmetry (reduced number of signals) due to a tricoordinate Ga center.

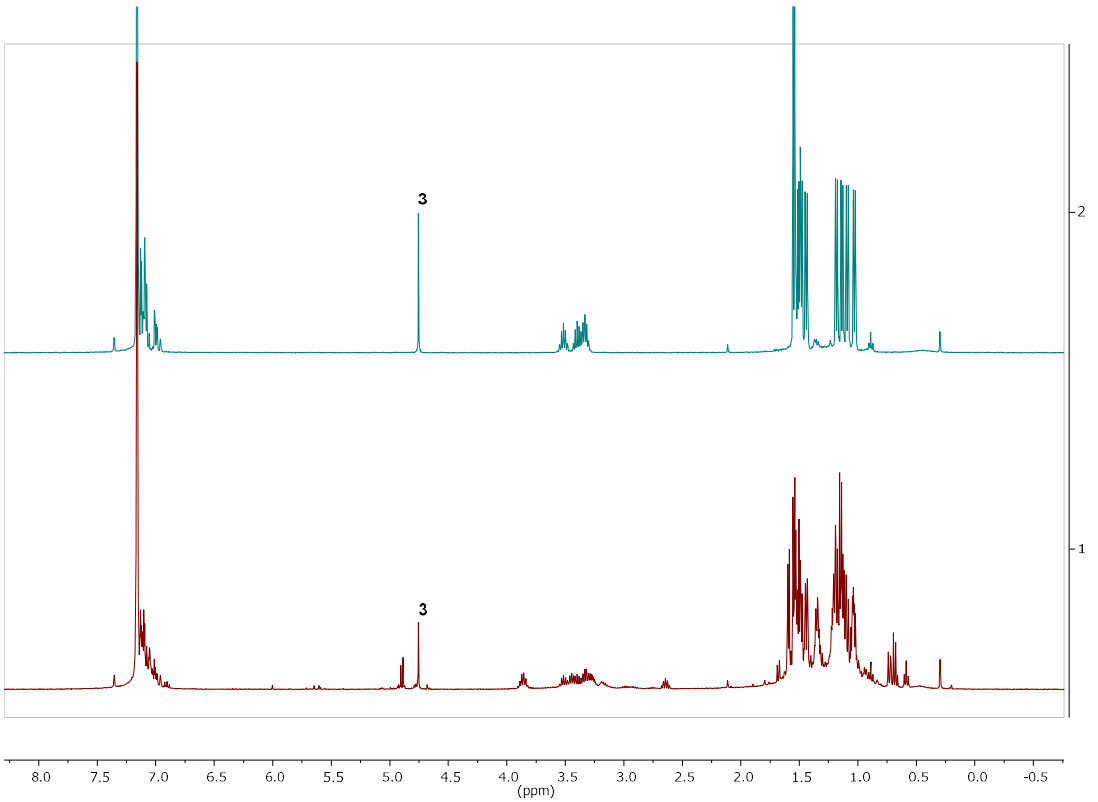

Fig. S 30. Top: ^{1}H NMR spectrum (400 MHz, C_6D_6, 25 °C) of the isolated crystals of L(Cl)Ga(C_4Cl_5) (**3**). Bottom: ^{1}H NMR spectrum (400 MHz, C_6D_6, 25 °C) of the sticky oily residue obtained by removing most of the volatiles of the mother liquor of the same batch.

B) Crystallographic Details

Table S2a. Crystallographic data of LGa(C_6H_{10}) (**1**), LGa($C_8H_{16}O_2Si$) (**2**), L(Cl)Ga(C_4Cl_5) (**3**), and L(Cl)In(C_4Cl_5) (**4**).

	1	**2**	**3**	**4**
Empirical formula	$C_{35}H_{51}GaN_2$	$C_{37}H_{57}GaN_2O_2Si$	$C_{33}H_{41}Cl_6GaN_2$	$C_{33}H_{41}Cl_6InN_2$
M	569.49	659.65	748.10	793.20
Crystal size [mm]	0.300 × 0.217 × 0.079	0.187 × 0.122 × 0.078	0.276 × 0.110 × 0.064	0.266 × 0.230 × 0.068
T [K]	100(2)	100(2)	100(2)	100(2)
Crystal system	triclinic	orthorhombic	orthorhombic	monoclinic
Space group	$P\bar{1}$	$P2_12_12_1$	$Pnma$	$P2_1/n$
a [Å]	10.9840(7)	8.9454(4)	16.2465(13)	9.3195(5)
b [Å]	11.0508(7)	18.5531(9)	20.9753(18)	39.215(2)
c [Å]	14.5148(9)	21.6447(11)	10.2454(9)	10.4654(6)
α [°]	87.870(3)	90	90	90
β [°]	77.262(3)	90	90	110.4368(16)
γ [°]	71.943(3)	90	90	90
V [Å^3]	1632.91(18)	3592.3(3)	3491.4(5)	3584.0(3)
Z	2	4	4	4
D_{calc} [g·cm-3]	1.158	1.220	1.423	1.470
μ(Mo/CuK$_\alpha$) [mm^{-1}]	0.866	1.612	1.273	9.574
Transmissions	0.75/0.68	0.75/0.62	0.75/0.67	0.75/0.41
F(000)	612	1416	1544	1616
Index ranges	$-18 \le h \le 18$	$-9 \le h \le 11$	$-25 \le h \le 25$	$-11 \le h \le 11$
	$-18 \le k \le 18$	$-23 \le k \le 23$	$-32 \le k \le 32$	$-49 \le k \le 49$
	$-24 \le l \le 24$	$-27 \le l \le 27$	$-15 \le l \le 15$	$-12 \le l \le 13$
θ_{max} [°]	36.461	80.411	33.242	79.388
Refl. collected	109502	80154	80839	127565
Independ. refl.	15946	7841	6848	7758
R_{int}	0.0342	0.0641	0.0444	0.0788
Refined parameters	355	403	228	423
R_1 [$I > 2\sigma(I)$]	0.0284	0.0258	0.0329	0.0441
wR_2 [all data]	0.0774	0.0656	0.0865	0.1231
x(Flack)		0.350(16)		
GooF	1.052	1.059	1.105	1.041
$\Delta\rho_{final}$ (max/min) [e·Å^{-3}]	0.686/-0.318	0.376/-0.277	1.617/-0.454	2.188/-1.341

Table S2b. Crystallographic data of L(Cl)Ga($CH_2C_6H_5$) (**5**), L(Cl)In($CH_2C_6H_5$) (**6**), and [LGa($CH_2C_6H_5$)][$B(C_6F_5)_4$] (**10**).

	5	**6**	**10**
Empirical formula	$C_{36}H_{48}ClGaN_2$	$C_{36}H_{48}ClInN_2$	$C_{67.14}H_{56.29}BCl_{0.29}F_{20}GaN_2$
M	613.93	659.03	1361.93
Crystal size [mm]	0.539 × 0.230 × 0.201	0.227 × 0.157 × 0.063	0.427 × 0.141 × 0.062
T [K]	100(2)	100(2)	100(2)
Crystal system	triclinic	triclinic	triclinic
Space group	$P\bar{1}$	$P\bar{1}$	$P\bar{1}$
a [Å]	10.2314(5)	10.2221(6)	13.7670(9)
b [Å]	12.1118(6)	12.3282(5)	15.1367(10)
c [Å]	14.0097(7)	14.0999(7)	17.3962(11)
α [°]	84.191(2)	81.527(4)	113.966(3)
β [°]	83.526(2)	86.405(4)	94.047(3)
γ [°]	72.750(2)	72.766(3)	109.063(3)
V [Å^3]	1643.22(14)	1678.23(15)	3043.0(4)
Z	2	2	2
D_{calc} [g·cm-3]	1.241	1.304	1.486
μ(Mo/CuK_α) [mm^{-1}]	0.945	6.537	0.570
Transmissions	0.75/0.62	0.75/0.46	0.75/0.68
F(000)	652	688	1388
Index ranges	$-17 \le h \le 17$	$-13 \le h \le 13$	$-21 \le h \le 21$
	$-20 \le k \le 20$	$-15 \le k \le 14$	$-23 \le k \le 23$
	$-23 \le l \le 23$	$-18 \le l \le 18$	$-26 \le l \le 26$
θ_{max} [°]	36.491	80.581	33.416
Refl. collected	178070	87957	265924
Independ. refl.	16108	7274	23521
R_{int}	0.0355	0.0542	0.0550
Refined parameters	371	371	860
R_1 [$I > 2\sigma(I)$]	0.0296	0.0194	0.0433
wR_2 [all data]	0.0816	0.0520	0.1142
x(Flack)			
GooF	1.135	1.068	1.061
$\Delta\rho_{final}$ (max/min) [e·Å^{-3}]	1.031/-0.430	0.558/-0.663	1.582/-0.622

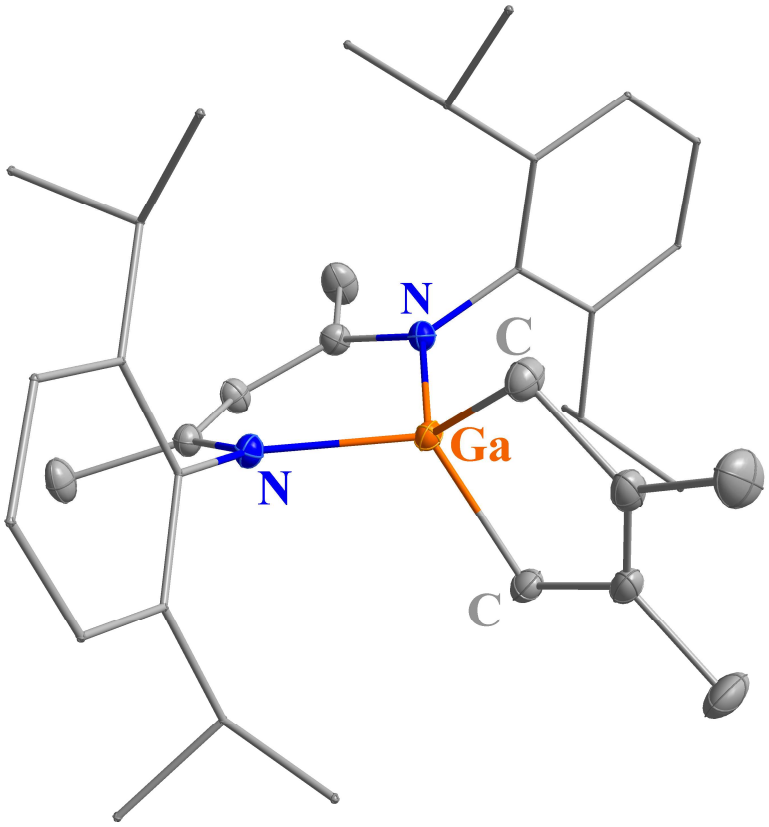

Fig. S31. Molecular structure of $LGa(C_6H_{10})$ (**1**) in the crystal. H atoms are omitted for clarity and displacement ellipsoids are drawn at the 50% probability level. The 2,6-diispropylphenyl group is displayed as a wireframe. Obtained from concentrated benzene solution upon storage at 7°C.

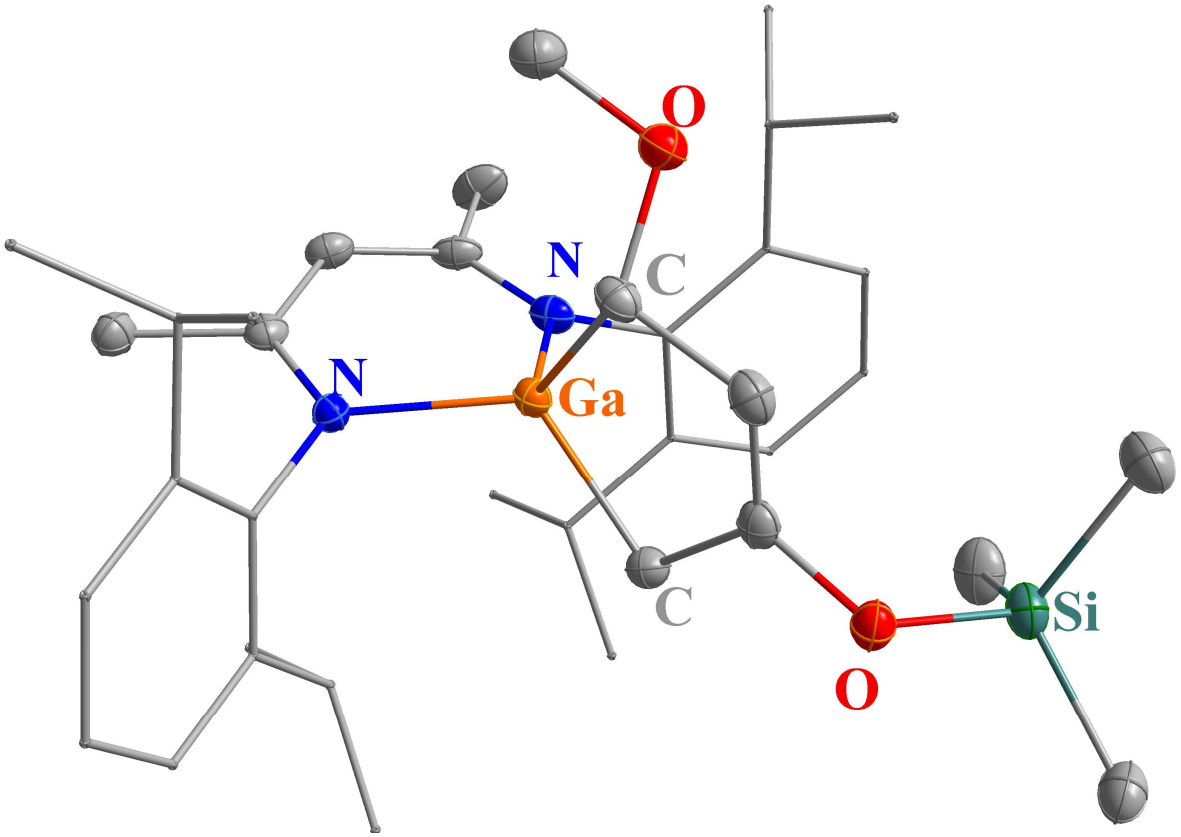

Fig. S32. Molecular structure of $LGa(C_8H_{16}O_2Si)$ (**2**) in the crystal. H atoms are omitted for clarity and displacement ellipsoids are drawn at the 50% probability level. The 2,6-diispropylphenyl group is displayed as a wireframe.

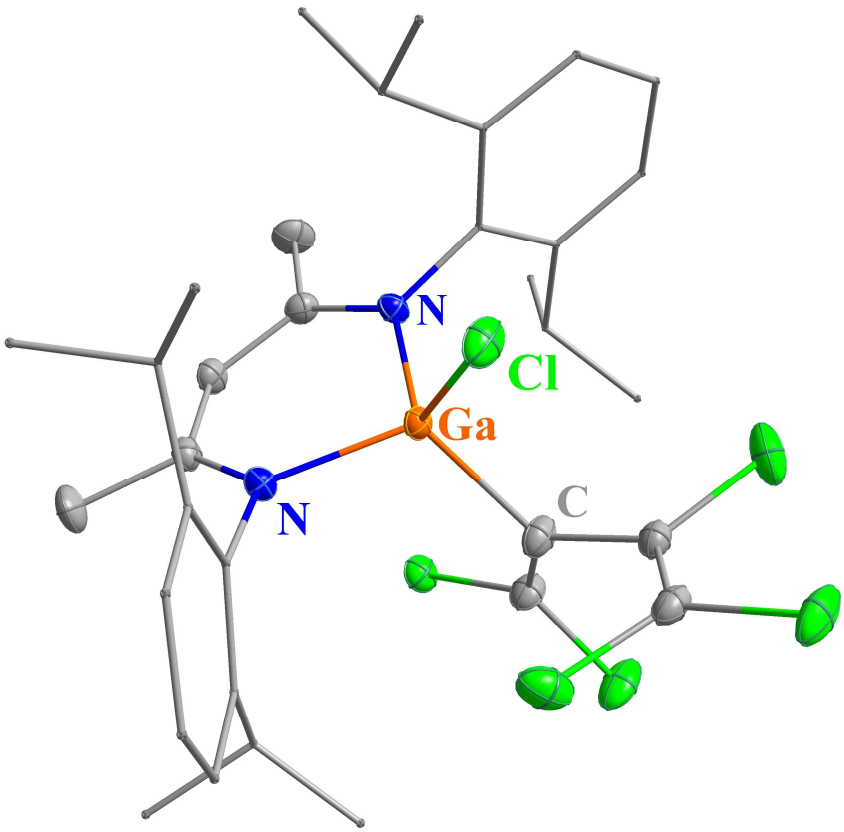

Fig. S33. Molecular structure of L(Cl)Ga(C_4Cl_5) (**3**) in the crystal. H atoms are omitted for clarity and displacement ellipsoids are drawn at the 50% probability level. Only one part of the disordered $ClCCl_2$ group is displayed. The 2,6-diispropylphenyl group is displayed as a wireframe.

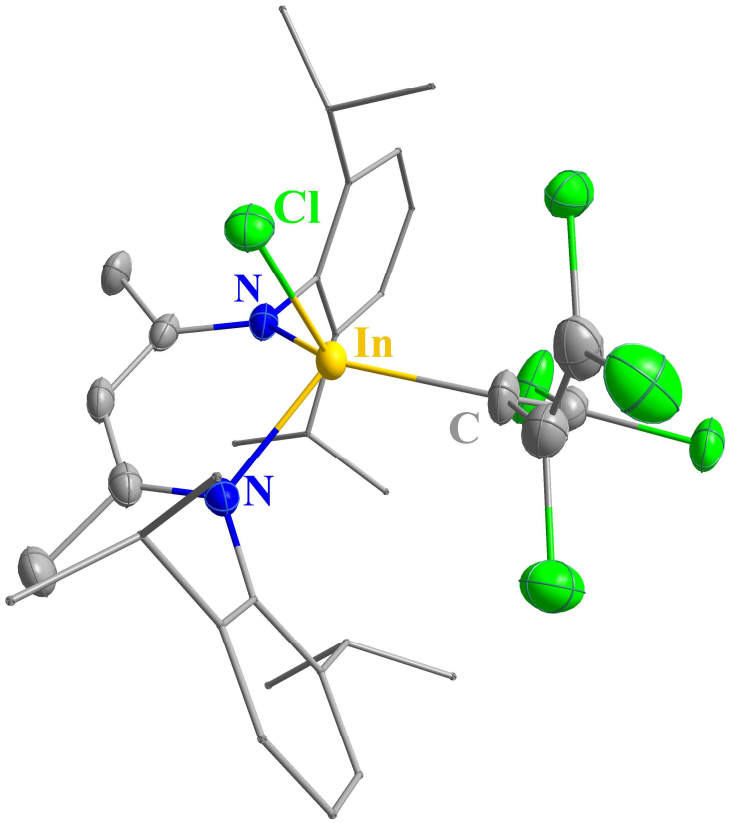

Fig. S34. Molecular structure of L(Cl)In (C_4Cl_5) (**4**) in the crystal. H atoms are omitted for clarity and displacement ellipsoids are drawn at the 50% probability level. Only the major component of the disordered $ClCCl_2$ group is displayed. The 2,6-diispropylphenyl group is displayed as a wireframe.

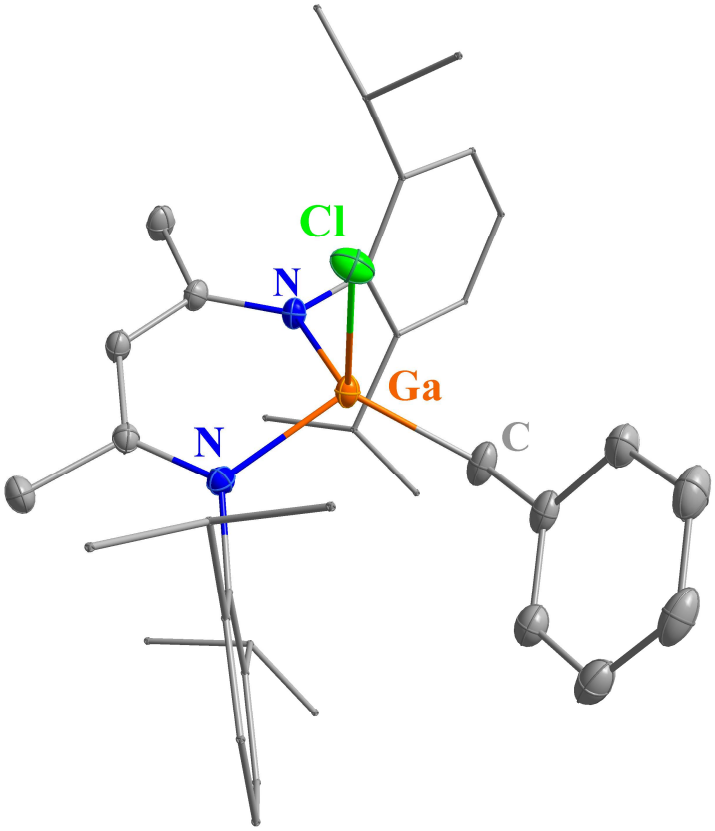

Fig. S35. Molecular structure of L(Cl)Ga($CH_2C_6H_5$) (**5**) in the crystal. H atoms are omitted for clarity and displacement ellipsoids are drawn at the 50% probability level. The 2,6-diispropylphenyl group is displayed as a wireframe.

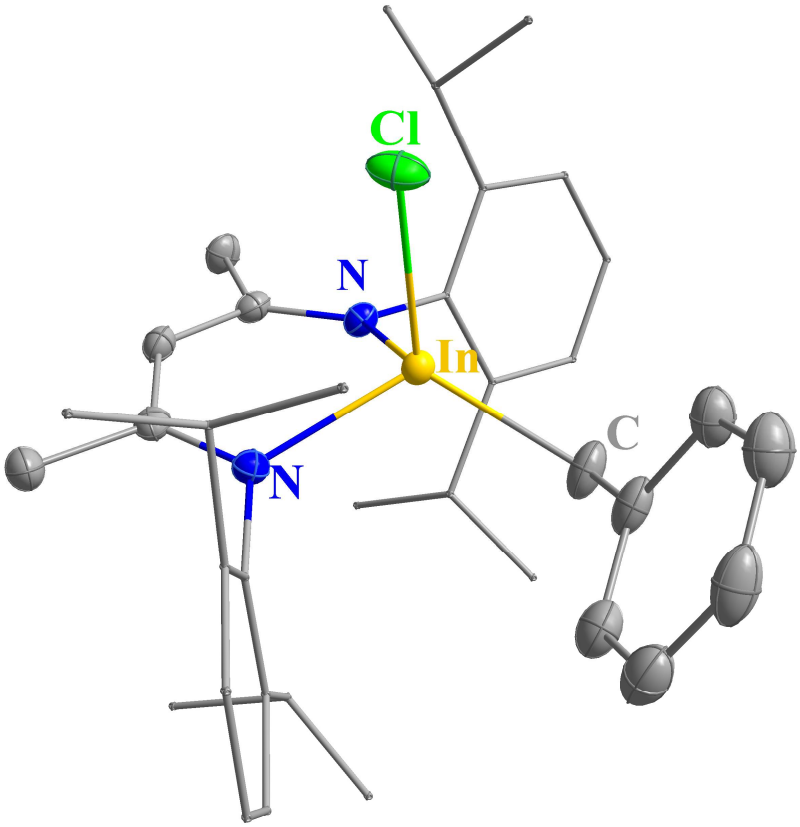

Fig. S36. Molecular structure of L(Cl)In($CH_2C_6H_5$) (**6**) in the crystal. H atoms are omitted for clarity and displacement ellipsoids are drawn at the 50% probability level. The 2,6-diispropylphenyl group is displayed as a wireframe.

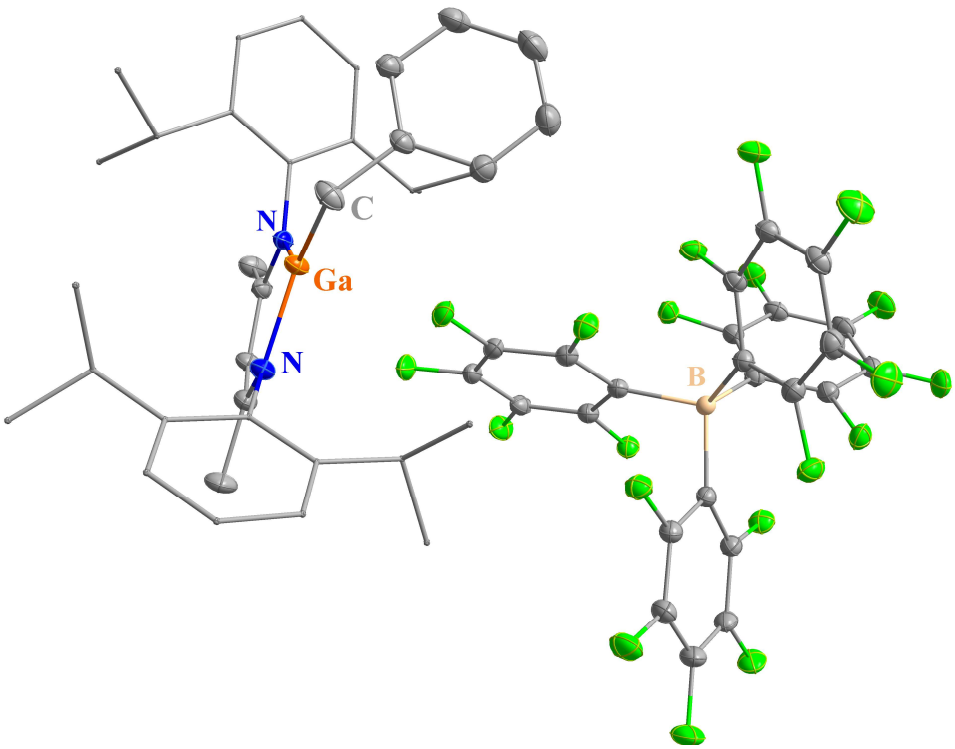

Fig. S37. Molecular structure of and [LGa($CH_2C_6H_5$)][B(C_6F_5)$_4$] (**10**) in the crystal. H atoms are omitted for clarity and displacement ellipsoids are drawn at the 50% probability level. The 2,6-diispropylphenyl group is displayed as a wireframe.